ELSEVIER

Contents lists available at ScienceDirect

Gondwana Research

journal homepage: www.elsevier.com/locate/gr



Research Paper



The late Ediacaran to early Cambrian subduction-related granitic magmatism of the Pampean orogen: Geochemical and isotopic constraints on hybridization processes

Priscila S. Zandomeni ^a, Juan A. Moreno ^{b,c,*}, Matías M. Morales Cámera ^{a,d}, Sebastián O. Verdecchia ^{a,d}, Edgardo G. Baldo ^{a,d}, Juan.A. Dahlquist ^{a,d}, César Casquet ^e, Miguel A.S. Basei ^f, Gilmara Santos da Cruz ^{a,d}, Carlos W. Rapela ^g

- a Facultad de Ciencias Exactas, Físicas y Naturales, Universidad Nacional de Córdoba, Av. Vélez Sarsfield 1611, X5016CGA Córdoba, Argentina
- ^b Departamento de Ciencias de la Tierra, Universidad de Huelva, 21071 Huelva, Spain
- ^c Centro de Investigación en Química Sostenible (CIQSO), Universidad de Huelva, 21071, Huelva, Spain
- d Centro de Investigaciones en Ciencias de la Tierra, Consejo Nacional de Investigaciones Científicas y Técnicas, Ingeniero Ismael Bordabehere y Av. Haya de la Torre, Ciudad Universitaria, X5016GCA Córdoba, Argentina
- ^e Departamento de Mineralogía y Petrología, Facultad de Ciencias Geológicas, Universidad Complutense (UCM), 28040 Madrid, Spain
- ^f Instituto de Geociências, Universidade de São Paulo, Rua do lago 562, São Paulo, SP 05508-080, Brazil
- g Centro de Investigaciones Geológicas (CIG), CONICET, Universidad Nacional de la Plata, Diagonal 113 N 275, 1900 La Plata, Argentina

ARTICLE INFO

ABSTRACT

Keywords:
Continental arc magmatism
Pampean orogen
Granite petrogenesis
Hybridization
Puncoviscana Series

The late Ediacaran to early Cambrian Pampean magmatic arc in Argentina represents an excellent example of subduction-related magmatism and continental crust formation. This study presents new geochemical, isotopic, and geochronological data from the Guasayán intrusive complex, which is a significant body within this magmatic arc. The data are integrated with a comprehensive compilation of published data from the arc elsewhere. The Pampean arc exhibits a wide range of rocks, from metaluminous I-type diorites to strongly peraluminous S-type granites, with the majority displaying hybrid compositions (mostly magnesian, calc-alkalic and slightly peraluminous compositions). Zircon U-Pb geochronology indicates that the Guasayán granitoids were emplaced mainly during a flare-up of arc magmatism between ca. 530 and 535 Ma. However, the presence of zircon antecrysts with ages of ca. 545 Ma in most of the Pampean arc granitoids, suggests that the magmatic system was long-lived, and the early crystallized zircon crystals were recycled into younger magmatic pulses. Geochemical and isotope data (Sr-Nd-Hf) highlight the interaction between mantle-derived magmas and crustal components, with magma mixing identified as the dominant process in the generation of the hybrid granitoids. Local-scale processes such as crustal assimilation, fractional crystallization, and peritectic entrainment also contributed to the geochemical and isotopic diversity. The involvement of the Puncoviscana Series as the crustal component of the mixed magmas is evidenced by zircon inheritance patterns and isotopic signatures. This study underscores the importance of magma mixing in the evolution of the Pampean arc and provides insights into the geodynamic processes driving continental crust formation in subduction-related settings.

1. Introduction

Magmas produced in magmatic arcs related to the subduction of oceanic slabs represent immense accumulations of intermediate calcalkaline igneous rocks (e.g., Ducea et al., 2015a). These magmas are primarily produced through the subduction of oceanic lithosphere, which introduces water and volatiles into the mantle wedge, triggering

partial melting and the production of basaltic magmas (Stern, 2002a; Tatsumi, 2005). Several studies conducted in recent years (e.g., DeCelles et al., 2009; Ducea et al., 2015b; Kirsch et al., 2016; Chapman et al., 2021; Ma et al., 2022, and references therein), suggest that these magma accumulations seem to occur cyclically over extended periods of time. These cycles include relatively short periods of high magma production (flare-ups), during which 75–80 % of the magmatic arc mass is

E-mail address: juanantonio.moreno@dct.uhu.es (J.A. Moreno).

https://doi.org/10.1016/j.gr.2025.09.012

^{*} Corresponding author.

generated in ca. 10–15 million years, separated by long intervals (around 25 to 70 million years) of low or no magma production (lulls).

The petrogenesis of granitic magmas in continental arcs is highly complex due to their hybrid nature (e.g., Castro, 2014), involving processes such as fractional crystallization (Annen et al., 2006), crustal assimilation (DePaolo, 1981; Beard et al., 2005), magma mixing (Barbarin, 2005), partial melting of the crust (Dahlquist et al., 2022), and/or possible involvement of heterogeneous sources (e.g., Grove et al., 2002; Castro et al., 2010). Furthermore, most modern trenches in arcs are erosive (e.g., Clift and Vannucchi, 2004; Stern, 2011), thus processes such as subduction erosion (Stern, 2011; 2020), tectonic underplating (Ducea et al., 2009) and relamination (Hacker et al., 2011) must be considered as likely mechanisms that introduce sediments and other crustal material into the root of arcs and the upper plate (Ducea et al., 2015b), contributing to the geochemical diversity of arc magmas (Castro et al., 2010; Ducea et al., 2017; Rojo-Pérez et al., 2022).

The formation of large silicic batholiths mainly of granodiorite to tonalite compositions, so-called Cordilleran-type batholiths, is often associated with periods of crustal thickening and magmatic flare-ups, during which large volumes of intermediate to felsic magmas are produced (Ducea and Barton, 2007; Ducea et al., 2015a; DeCelles et al., 2009). These contribute to the recycling of crustal material and the generation of hybrid magmas with distinct geochemical and isotopic signatures (Ducea et al., 2017; Lee et al., 2012). Furthermore, this is consistent with the fact that most granitic batholiths, whether in subduction or collisional settings, exhibit a hybrid character (Castro et al., 1991). Thus, integrated studies of petrography, field relationships, whole-rock geochemistry, and isotope systematics in arc granites are critical to constrain the role of mixing processes (Zhang et al., 2016) in the genesis of Cordilleran-type granitoids—key to deciphering the formation and evolution of continental crust.

The late Ediacaran to Early Cambrian Pampean orogen of SW Gondwana (Argentina) records magmatism that remains poorly understood due to its geographical fragmented lithotectonic domains (Fig. 1) and unclear relationships, obscured in the west of Argentina by late Cambrian to early Carboniferous orogens. The granitic magmatism associated with the Pampean arc exhibits a wide range of compositions, from metaluminous I-type granitoids to strongly peraluminous S-type granites, suggesting complex petrogenetic processes involving both mantle and crustal sources (Lira et al., 1997; Suzaño et al., 2015; Dahlquist et al., 2016; Ortiz et al., 2017).

Most Pampean arc granitoids show a hybrid nature (Dahlquist et al., 2016; Zandomeni et al., 2021; Bellos et al., 2024), although the petrogenesis of the arc as a whole remains unresolved. Despite similarities across the different igneous complexes (from Northwest Argentina, Eastern Sierras Pampeanas and the North Patagonian Massif) processes critical to arc evolution, such as subduction erosion, are largely unexplored in the Pampean context. Here we present new geochemical, isotopic, and geochronological data for granitoids from Sierra de Guasayán (eastern Sierras Pampeanas, Argentina), integrated with published data from other Pampean arc outcrops elsewhere, to constrain magma sources, petrogenetic mechanisms, and their geodynamic significance for the assembly of Gondwana.

2. The Pampean orogeny in the SW margin of Gondwana

The early evolution of the SW margin of Gondwana in southern South America was linked to the development of two subsequent orogenic belts, Pampean and Famatinian, first recognised by Aceñaloza and Toselli (1976). The Pampean orogeny, which involved the development of a magmatic arc followed by continental collision, took place during the amalgamation of Gondwana, between ca. 545 and 515 Ma (e. g., Rapela et al., 1998, 2016; Casquet et al., 2018), although other authors considered an earlier start at ca. 555 Ma (Schwartz et al., 2008). On the other hand, the Famatinian orogeny was linked to a new subduction stage in the western margin of Gondwana with associated

magmatism, sedimentation, metamorphism and deformation, occurring between 500 and 410 Ma (Rapela et al., 2018; Otamendi et al., 2020, Casquet et al., 2021).

The Pampean orogeny is an important event, characterized by arcrelated magmatism and regional metamorphism and anatexis, recorded in the Sierras Pampeanas, Puna, Cordillera Oriental and Patagonia (Fig. 1). The Pampean orogeny was almost coeval with other orogenies that brought about the amalgamation of Gondwana such as the Saldania (South Africa, Rozendaal et al., 1999; Curtis, 2001; Chemale et al., 2011), Delamerian (Australia, Foden et al., 2006) and Ross orogenies (Antarctica, Stump, 1995; Goodge, 1997), in which similar geological processes have been reported. Moreover, some authors have proposed that the Pampean and Saldania belts were probably juxtaposed before large right-lateral displacement along the Transbrasiliano Lineament in Cambrian and later times (Casquet et al., 2018).

There are different hypotheses that try to explain the variety of rocks, the volume of continental crust and the structure of the Pampean orogeny (see Ramos et al., 2014). Some of the main hypotheses are based on collisional models between different blocks, e.g. the MARA block (Maz, Arequipa, Antofalla, Casquet et al., 2012, 2018) against the Kalahari Craton under an initial oblique subduction regimen (Rapela et al., 2007; Siegesmund et al., 2010; Casquet et al., 2012, 2018) or the Pampia Terrane (Ramos and Vujovich, 1993) against the Río de la Plata Craton in an orthogonal regime (see Ramos et al., 2014). Alternatively, Escayola et al. (2007) proposed an island arc that first collided in the Neoproterozoic with the Río de la Plata Craton under an initial westward subduction and followed by collision of Pampia Terrane (see Ramos et al., 2015). A non-collisional hypothesis invoked the subduction of a mid-oceanic ridge and its interaction with an accretional prism (Gromet and Simpson, 2000; Simpson et al., 2003; Gromet et al., 2005; Tibaldi et al., 2008; Von Gosen and Prozzi, 2010). Whereas the Pampean orogeny is interpreted as a discrete cycle (see review in Rapela et al., 2016; Casquet et al., 2018; Otamendi et al., 2020), other authors consider the Pampean orogeny as part of a continuous process along the SW margin of Gondwana from Ediacaran to Mid-Paleozoic time (Lucassen et al., 2000; Weinberg et al., 2018).

Evidence of the Pampean orogeny is recognised in South America from north to south of Argentina, not only in Sierras Pampeanas. In Northwest Argentina (Puna, Cordillera Oriental and part of northern Sierras Pampeanas as Sierras de Guasayán and Tafi del Valle) there are well recognised outcrops, while in Patagonia it is exclusively found in the North Patagonian Massif (Pankhurst et al., 2014). The outcrops where the Pampean orogen is best preserved are: 1) the northern part of the Sierras Chicas de Córdoba (Rapela et al., 1998); 2) the Sierra Norte-Ambargasta (von Gosen et al., 2014; Iannizzotto et al., 2013); 3) Sierra de Guasayán (Dahlquist et al., 2016; Zandomeni et al., 2017b); 4) the Puna and Cordillera Oriental in the NOA (Northwest Argentina; Hongn et al., 2010; Hauser et al., 2011; Suzaño et al., 2017), and 5) as an inlier within the Famatinian belt (Late Cambrian - Early Devonian orogen; Rapela et al., 2018; Casquet et al., 2021) away from the former ones (Larrovere et al., 2021) (Fig. 1). These outcrops represent different lithotectonic domains of the original Pampean orogen that we can recognise as essentially: 1) the magmatic arc domain and 2) the collisional belt (see below). The Pampean orogen ends abruptly against the Córdoba Fault in the east, which suggests that it extended further east (current coordinates) before the fault displaced part of it. We have interpreted the Córdoba fault as a large cortical-scale structure probably a continuation of the Transbrasiliano Lineament (TBL) (Cordani et al., 2003) based on geological and geophysical evidence (Rapela et al., 2007; Favetto et al., 2015). The fault juxtaposed the Rio de la Plata craton with the inner zone of the Pampean orogen by displacing rightlaterally the eastern part that is now missing in South America. Casquet et al. (2018) proposed that the missing part is the Saldania belt that fringes the south of the Kalahari craton in South Africa. In fact, the Saldania belt shares many features in common with the Argentine Pampean belt such as stratigraphy, magmatism and chronology

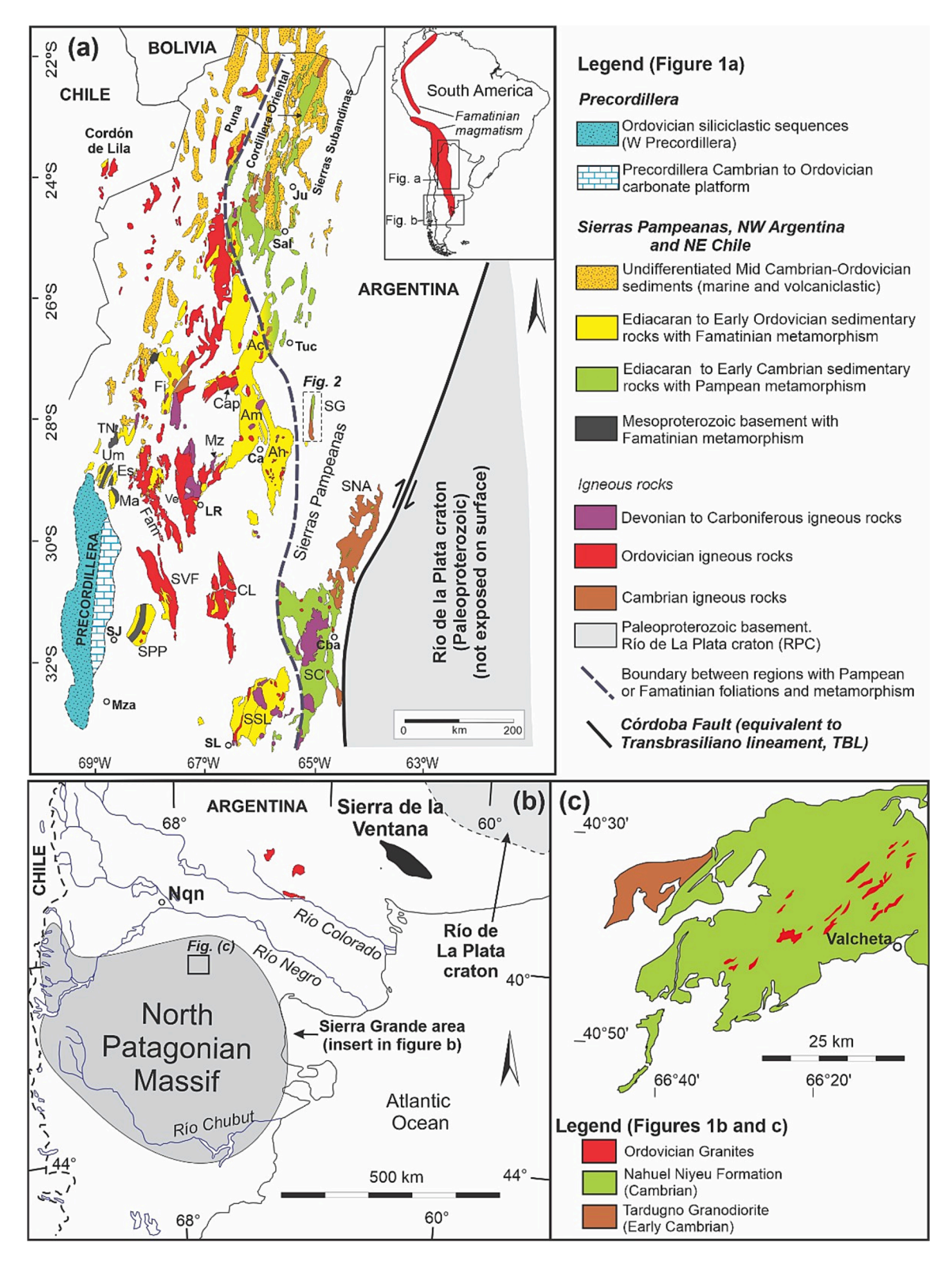


Fig. 1. A) Early Paleozoic geology of the Sierras Pampeanas, Precordillera, Puna, Cordillera Oriental and Sierras Subandinas. EPEB: Eastern Puna Eruptive Belt. Main ranges are indicated: Sierra de Aconquija (Ac), Sierra de Ambato (Am), Sierra de Ancasti (An), Sierra de Belén (Be), Sierra de Capillitas (Cap), Sierra del Espinal (Es), Sierra de Famatina (Fam), Sierra de Fiambalá (Fi), Sierras de Chepes-Los Llanos (CL), Sierra de Maz (Ma), Sierra de Mazán (Mz), Sierra de Córdoba (SC), Sierra Norte-Ambargasta (SNA), Sierra de Pie de Palo (SPP), Sierra de San Luis (SSL), Sierra del Toro Negro (TN), Sierra de Valle Fértil (SVF), Sierra de Velasco (Ve), Sierra de Umango (Um). Town localities: Jujuy (Ju), Salta (Sal), Tucumán (Tuc), Catamarca (Ca), La Rioja (LR), San Juan (SJ), Córdoba (Cba), Mendoza (Mza), San Luis (SLo). Modified from Rapela et al. (2018). B) Sketch map of northeastern Patagonia showing the Early Paleozoic units in the Río Colorado and the location of the Valcheta area (modified from Rapela et al., 2018). Nqn: Neuquén. C) Early Paleozoic units of the Valcheta area (modified from Rapela and Pankhurst, 2020).

(Casquet et al., 2018).

Regarding the geological history recorded in the Sierras de Córdoba, the Pampean orogeny began with the development of a Late Ediacaran to Early Cambrian continental calc-alkaline arc (541–523 Ma) emplaced in the metasedimentary Puncoviscana Series (Casquet et al., 2018, and references therein). This was followed by a continental collision leading to crustal thickening with strong folding accompanied by penetrative foliation, shearing, and low- to high-grade regional metamorphism of the Puncoviscana Series, accompanied by anatexis with the generation of S-type granites at ca. 525 Ma (Rapela et al., 2007; Casquet et al., 2018 and references therein).

Various ultrabasic and basic rocks have been recognised in the Sierras de Córdoba (Eastern Sierras Pampeanas) (e.g., Villar, 1975; Mutti, 1997; Rapela et al., 1998; Escayola et al., 2007; Anzil and Martino, 2009). Amphibolites with MORB signature, but without a clearly defined origin and reliable ages, were described by Rapela et al. (1998). On the other hand, Tibaldi et al. (2021) found a variety of basic and ultrabasic rocks of ca. 520 Ma in southern Sierras de Córdoba, including mafic to intermediate alkaline OIB-like rocks, mafic tholeiitic N-MORB rocks, transitional mafic rocks, and minor trondhjemitic rocks with adakitic geochemical signature. The last are not related to the Cordilleran-type magmatic arc and likely resulted from later processes in the Pampean orogen (Tibaldi et al., 2021), although these authors explained them through the interaction between oceanic ridge and accretionary prism in a convergent margin. Furthermore, the ultrabasic rocks have been interpreted either as scales from the mantle that intercalated within the accretionary prism (Martino et al., 2010), or as relicts of a dismembered ophiolite (e.g., Ramos et al., 2000; Escayola et al., 2007; Proenza et al., 2008, and references therein), thus representing the Pampean collisional suture (Escayola et al., 2007; Casquet et al., 2018, and references therein). Therefore, it seems that no subduction-related basic or ultrabasic rocks linked to the Pampean arc have been reported so far.

2.1. The Ediacaran to Cambrian metasedimentary successions

Two metasedimentary successions were involved in the Pampean orogeny: the Puncoviscana Series and the Ancaján Series (see summaries in Rapela et al., 2016). The Puncoviscana Series is represented by low-to high-grade metasedimentay rocks, including the Puncoviscana Formation (Turner, 1960). This latter is widely exposed in northwest Argentina and is mainly composed of a thick low-grade succession of siliciclastic (metaturbidites and minor calcsilicate levels) as well as volcanic beds (Jezek, 1990; Omarini et al., 1999; Zimmermann, 2005; Aceñolaza and Aceñolaza, 2007; Escayola et al., 2011). Its nature and tectonic setting are controversial as it is considered as formed in a passive margin, a forearc basin or a rift (see the reviews in Casquet et al., 2018; Weinberg et al., 2018). Rocks with pattern of detrital zircon ages similar to the Puncoviscana Formation from northwest Argentina were recognised in the Eastern Sierras Pampeanas, where they form extensive outcrops of migmatites and minor low-grade metamorphic rocks (Rapela et al., 2007, 2016; Escayola et al., 2007; Murra et al., 2011, 2016; Iannizzotto et al., 2013), and integrated as part of the Puncoviscana Series. The Puncoviscana Series shows characteristic almost bimodal detrital zircon populations represented by major age peaks at 1100-960 Ma and 680-570 Ma, along with proportionally minor ages of 1.7-2.0 Ga and ca. 2.6 Ga (Adams et al., 2010; Escayola et al., 2011; Rapela et al., 2016, and references therein). A characteristic feature is the absence of zircon grains with ages of 2.02-2.26 Ga typical of the Río de la Plata Craton (Rapela et al., 2007). The Puncoviscana Series would be deposited between 570 and 537 Ma (Rapela et al., 2007, 2016; Escayola et al., 2011; Iannizzotto et al., 2013; Aparicio González et al., 2014; Casquet et al., 2018). Younger ages have also been attributed to the Puncoviscana Series (Adams et al., 2008, 2011) that resulted from the erosion of an early Pampean magmatic arc (see Weinberg et al., 2018). However, the latter have better been included in a different sedimentary succession, i.

e., the post-Pampean sedimentary series (Verdecchia et al., 2011; Rapela et al., 2016; Ramacciotti et al., 2018). The detrital zircon age patterns of the Puncoviscana Series indicate derivation from Gondwanan sources (see Adams et al., 2008; Rapela et al., 2016).

The Ancaján metasedimentary Series was identified in the Sierras Pampeanas and is represented by medium- to high-grade rocks composed of marbles and metasiliciclastic rocks (Murra et al., 2011, 2016; Rapela et al., 2016). An Ediacaran sedimentation age was constrained from Sr isotope compositions (Murra et al., 2011, 2016). The detrital zircon ages in the Ancaján Series are characterized by a conspicuous age distribution with peaks at ca. 0.9-1.5 Ga and ca. 1.8-1.9 Ga and less abundant ages at ca. 800 Ma. The absence of late Neproterozoic ages is the main difference from the Puncoviscana Series. Rapela et al. (2016) suggested a Laurentian origin for the Ancaján Series: it has been correlated with the Difunta Correa metasedimentary Series recognised further west, which shares the same Laurentia-derived zircon-age patterns (Ramacciotti et al., 2015).

3. The Pampean magmatic arc

The Pampean magmatic arc developed in Cambrian times during the early continental margin subduction phase of the Pampean orogeny. In southern South America, relicts of this magmatism can be recognised in Northwest Argentina at Puna, Cordillera Oriental, Eastern Sierras Pampeanas and Patagonia (southern Argentina in the North Patagonian Massif) (Lira et al., 1997; Rapela et al., 1998; Schwartz et al., 2008; Escayola et al., 2011; Hauser et al., 2011; Iannizzotto et al., 2013; von Gosen et al., 2014; Pankhurst et al., 2014; Suzaño et al., 2015, 2017; Dahlquist et al., 2016; Ortiz et al., 2017, 2019; Rapela and Pankhurst, 2020; Bellos et al., 2024). This igneous belt mainly consists of Cordilleran magnesian and calc-alkaline intermediate to felsic plutonic rocks (diorite to monzogranite) with metaluminous to peraluminous composition and constitutes the Cordilleran-type Pampean magmatic arc (e.g., Lira et al., 1997; Rapela et al., 1998; Ortiz et al., 2017; Casquet et al., 2018; Bellos et al., 2024). In the Eastern Sierras Pampeanas, this magmatic arc intruded the Puncoviscana Series (country rocks), creating in some cases a narrow aureole of contact metamorphism with development of cordierite-bearing hornfels (e.g., Sierra de Guasayán; Zandomeni et al., 2017a; Zandomeni et al., 2017b; Zandomeni et al. 2021). Subvolcanic and volcanic rocks (e.g., tuff) intercalated with metaclastic rocks have also been reported (see Escayola et al., 2011; von Gosen et al., 2014).

Recent works have reported the hybrid character of the Pampean arc granitoids (Suzaño et al., 2015, 2017, Ortiz et al., 2017, 2019; Zandomeni et al., 2021) with ϵNd_t values varying between +2 and -10 (Hauser et al., 2011; Iannizzotto et al., 2013; Pankhurst et al., 2014; Ortiz et al., 2017, 2019; Suzaño et al., 2017) and ϵHft values between -6.9 and +9.1 (Hauser et al., 2011; Pankhurst et al., 2014; Dahlquist et al., 2016; Ortiz et al., 2017, 2019), showing important and variable contribution of the continental crust in the genesis of these Cordilleran arc-related granitic rocks.

Large batholiths (Tastil and Sierra Norte-Ambargasta batholiths) and small plutons (e.g., Guasayán pluton) formed during the Pampean magmatic-arc activity. The granitoids from the Sierra Norte-Ambargasta and those from Cumbres Calchaquies have U-Pb zircon ages of 541 – 522 Ma (Schwartz et al., 2008; Siegesmund et al., 2010; Iannizzotto et al., 2013; Von Gosen et al., 2014., Bellos et al., 2020b). The Tastil batholith and other plutons from the Cordillera Oriental also yield similar U-Pb zircon ages in the range of 541 – 523 Ma (Hongn et al., 2010; Aparicio González et al., 2011; Hauser et al., 2011), whereas the igneous complexes from the Puna give younger Cambrian ages (521 – 503 Ma; Ortiz et al., 2017, 2019; Suzaño et al., 2017, and references therein). In addition, Cambrian granitoids with U-Pb zircon ages around 530 – 520 Ma were reported in the North Patagonian massif (Rapalini et al., 2013; Pankhurst et al., 2014), suggesting the extension and continuity of the arc magmatism south of the Río Colorado.

Additionally, recent studies have correlated the Pampean belt in South America with the Saldania belt, establishing a connection between the Pampean magmatism and the Pan-African Cape Granite Suite of South Africa (Casquet et al., 2018). This suite is characterized by voluminous S-type and minor I-type (syn- to late-tectonic) as well as A-type (post-tectonic) granites, with U-Pb zircon ages of approximately 550–510 Ma and peak plutonic activity between 540 and 530 Ma (Schoch, 1975; Scheepers, 1995; Da Silva et al., 2000; Scheepers and Schoch, 2006; Villaros et al., 2009, 2012; Chemale et al., 2011; Farina et al., 2012). This correlation highlights the widespread nature of arc magmatism during this period and suggests significant geodynamic links between South America and southern Africa.

4. Geological setting of the arc in the Sierra de Guasayán: The Guasayán intrusive complex

In the northern region of the Eastern Sierras Pampeanas, the Pampean magmatic arc crops out in a sub-meridional mountain range 76 km long known as Sierra de Guasayán (Beder, 1928; Fig. 2) which is the focus of this work. This sierra lies between northwestern Argentina (Puna, Cordillera Oriental) and the Sierra Norte-Ambargasta, the main exponents of the aforementioned magmatism, representing thus a link between the two (Dahlquist et al., 2016). In the Sierra de Guasayán a variety of granitic units are exposed, which include the Guasayán, El Escondido and El Martirizado plutons, as well as small-size igneous bodies as the La Soledad quartz diorite and Alto Bello granodiorite (Zandomeni et al., 2017b; Zandomeni et al. 2021). Subvolcanic acidic sills and minor basic dykes are also present. They were emplaced into a low- to mid-grade metamorphic basement developing narrow contact metamorphism aureoles (Zandomeni et al., 2017a). Dahlquist et al. (2016) reported a U-Pb zircon age of 533 \pm 4 Ma for the Guasayán pluton, which is consistent with the K-Ar colling ages in biotite (500 \pm 20 to 541 \pm 7 Ma) reported by González and Toselli (1974) and Omil (1992).

The main field relations and petrographic features of the different units are summarized as follows (see more details in Zandomeni et al., 2017b; Zandomeni et al. 2021):

- 1) The Guasayán pluton is a 170 km² undeformed granitoid body with a sharp contact with surrounding rocks, forming a metamorphic zone with cordierite, biotite, and K-feldspar hornfels. It contains metamorphic septa and rounded mafic microgranular enclaves (MME). Key features include biotite clots, subangular metamorphic xenoliths, and plagioclase-mantled K-feldspar phenocrysts with rapakivi texture. The main rock type is porphyritic biotite granodiorite to monzogranite, with K-feldspar phenocrysts oriented along a north–south magmatic foliation, set in an equigranular matrix made of plagioclase, quartz, alkali feldspar, and biotite. Accessory minerals include zircon, apatite, and ilmenite, while secondary minerals are chlorite, sericite, and epidote. The mafic enclaves are composed of plagioclase, quartz, biotite, and amphibole.
- 2) The El Escondido pluton is a small, subcircular body (~6.23 km²) in the northern Sierra de Guasayán. It was emplaced discordantly in the metamorphic basement, creating a thin metamorphic aureole with cordierite-biotite-K-feldspar hornfels. The pluton contains rectangular metamorphic xenoliths and rounded mafic enclaves. It is made up of medium-grained grey granodiorite with plagioclase, quartz, alkali feldspar, and biotite, alongside accessory minerals like allanite, monazite, zircon, apatite, and magnetite. At its edges, porphyritic facies are observed, with plagioclase and alkali feldspar phenocrysts featuring rapakivi texture. The enclaves are fine- to medium-grained, with tonalitic to granodioritic composition, containing plagioclase, quartz, biotite, amphibole, and various accessory minerals.
- 3) The El Martirizado pluton is a non-deformed red igneous formation situated in the northernmost region of the Sierra de Guasayán, spanning approximately 0.6 km². Its boundaries with the

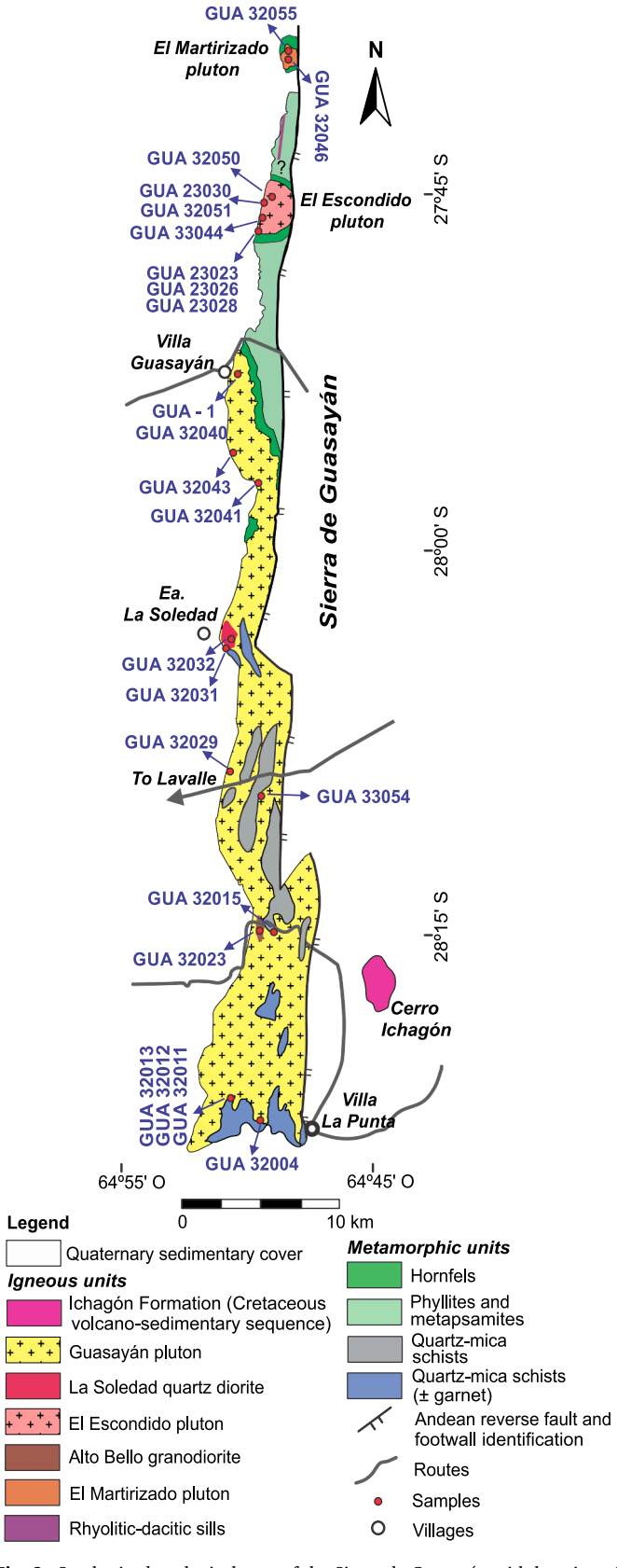


Fig. 2. Synthesized geological map of the Sierra de Guasayán with location of the studied samples and sample GUA-1 (Dahlquist et al., 2016).

surrounding rock are not clearly defined, and it is challenging to discern field relations due to the presence of vegetation and soil. The pluton consists of medium- to fine-grained, equigranular granodiorite to monzogranite, containing plagioclase, quartz, alkali feldspar, and biotite, as well as accessory minerals like monazite, zircon, apatite, and rutile. Common secondary minerals found include chlorite, magnetite, calcite, and fine-grained white mica. No evidence of metamorphic xenoliths or mafic enclaves was found.

- 4) The La Soledad quartz diorite appears as several isolated rounded blocks over an area of about 200 m², surrounded by the porphyritic biotite Guasayán pluton, though no contacts between them are visible. This rock is an equigranular medium- to fine-grained grey quartz diorite, primarily composed of plagioclase, quartz, biotite, pargasite, and alkali feldspar. Accessory minerals include titanite, zircon, apatite, and ilmenite, while common secondary minerals are chlorite, epidote, and fine-grained white mica.
- 5) The Alto Bello granodiorite is found in the southern section of the Sierra de Guasayán, represented by several isolated blocks across an area of approximately 500 m², bordered to the east by the porphyritic biotite Guasayán pluton, although their contact is not visible. The western outcrops are completely obscured by vegetation and soil. This rock is an equigranular, fine- to medium-grained grey granodiorite containing two micas and displaying internal mica foliation, with numerous metamorphic xenoliths aligned parallel to this foliation. The primary mineral composition of the granodiorite includes plagioclase, quartz, alkali feldspar, biotite, muscovite, cordierite, and sillimanite, with accessory minerals such as monazite, zircon, apatite, ilmenite, and rutile. Common secondary minerals are chlorite, pinite, epidote, and fine-grained white mica aggregates.

We include here granitoids which have biotite \pm amphibole (metaluminous or slightly peraluminous) (see below) and other peraluminous with Al-rich minerals (muscovite, cordierite, sillimanite). Both types are taken as the components of the Pampean magmatic arc, since they cluster and were emplaced almost coevally. Although they are minor in proportion, the clearly peraluminous granitoids are present in almost all arc-related Pampean plutons and batholiths (see descriptions and discussion below).

5. Samples and methods

For this study, we collected 21 samples of granitoids from the Sierra de Guasayán (Fig. 2): 11 from the main Guasayán pluton (including one mafic enclave), 7 from the El Escondido pluton (including one mafic enclave), one from the El Martirizado pluton, one from the La Soledad quartz diorite and one from the Alto Bello granodiorite. Whole-rock major and trace element compositions were determined for the complete set of samples (Supplementary Material S1), whereas 7 samples from the different units have also been analysed for Nd and Sr isotopes (Supplementary Material S1). For U-Pb zircon dating, zircon grains were separated from three granitic samples and one low-grade metapsammite sample of the country rock. Detailed information about the analytical procedures of the used methods is given in the Supplementary Material S2. Our results for the granitoids from the Sierra de Guasayán are completed with published data (geochemical, geochronological and isotope data) for one sample of the Guasayán pluton from Dahlquist et al. (2016), 3 samples of the Guasayán pluton and 2 samples of the El Escondido pluton from Bellos et al. (2020a).

5.1. Compositional database

An extensive database with compositional data of different Cambrian arc-related granitoids (Supplementary Material S3) have been compiled for comparison with the new data and to assess the petrogenetic processes that operated in the Pampean arc. The database consists of 137 samples of plutonic and volcanic rocks from the Sierras Pampeanas,

Cordillera Oriental, Puna and North Patagonian Massif. Samples with ${\rm SiO_2}$ higher than 74 wt%, which represent a minor population of the whole dataset, have not been included in the database, such highly differentiated compositions could obscure the effects of the main petrogenetic mechanisms working in the arc. All samples (n = 137) have major elements compositional data. 136 samples have trace element compositions, from which only 57 have complete REE data.

A total of 23 samples of granitoids with both Nd and Sr isotope data have also been compiled (Supplementary Material S4). In addition, Nd and Sr isotope data of samples of the Puncoviscana Series (n = 11) and Cambrian (Pampean) anatectic S-type granites (n = 14) related to the regional metamorphism were gathered for comparison with the Pampean subduction-related granitoids.

Finally, a database with zircon Hf isotope data of zircon grains with ages between 500 and 555 Ma has been assembled (n=78; Supplementary Material S4).

6. U-pb zircon ages

Three granitic samples and one metamorphic country rock were collected for geochronology (data in Supplementary Material S5): sample GUA-32004 from the southern part of the Guasayán pluton, sample GUA-32050 from the central area of the El Escondido pluton, GUA-32023 from the Alto Bello granodiorite and sample GUA-23062 (metapsammite) to the north of the Guasayán pluton (Fig. 2).

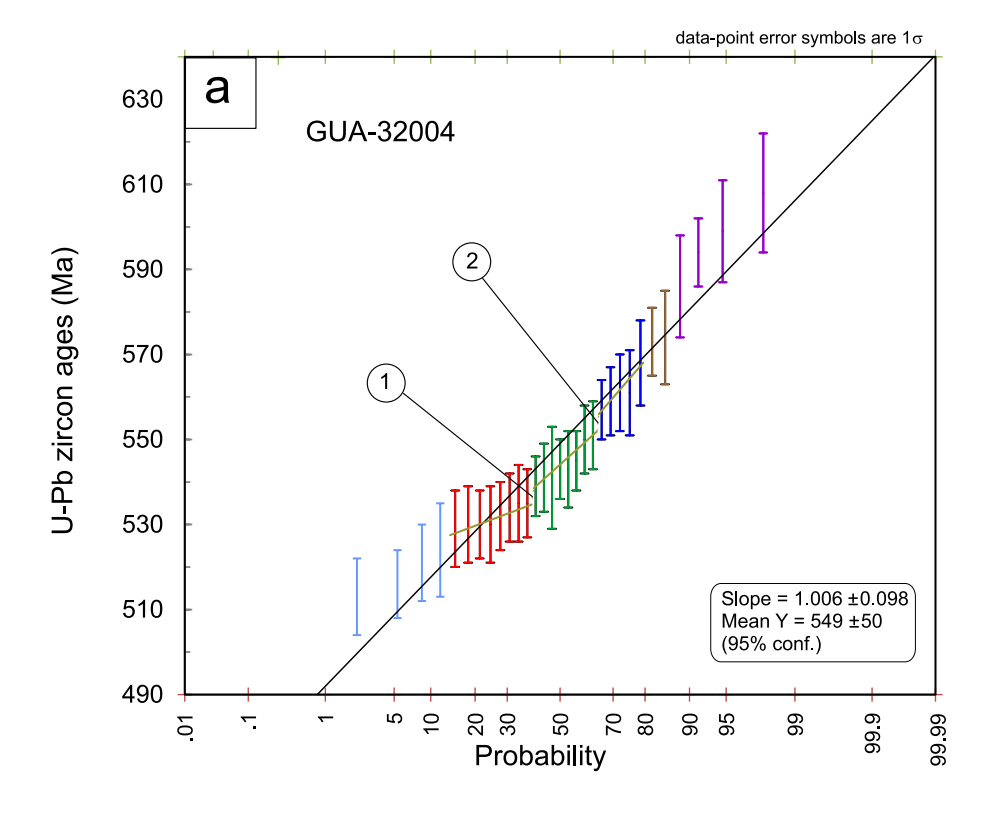
Zircon crystals from the granitic bodies are mostly euhedral to subhedral, prismatic with bipyramidal terminations. They have similar variable sizes around 100–500 μm long and up to 85 μm wide, although those from the Alto Bello granodiorite have a more limited length 130–170 μm and abundant rounded forms. Zircon grains mainly show oscillatory zoning and minor sector zoning, although patchy zoning has also been recognised in a few grains from the Alto Bello granodiorite (Supplementary Material S6).

Zircon grains from the metapsammite country rock are mainly euhedral to subhedral with prismatic elongated habits $100-200 \,\mu m$ long and $30-70 \,\mu m$ wide. Subrounded grains of $80-100 \,\mu m$ diameter have also been recognised. All zircon grains exhibit high luminescence, oscillatory zoning and less common sector zoning. Most grains have subhedral inherited cores and some of them show reabsorption textures rounded by rims with oscillatory zoning (Supplementary Material S6).

Analyses in samples from the Guasayán and El Escodindo plutons concentrated in rims, although a few cores were also analysed, whereas analyses in the Alto Bello granodiorite and the metasedimentary rock were carried out systematically in both rims and cores.

6.1. Guasayán pluton (GUA-32004)

A total of 36 LA-MC-ICP-MS U-Pb analyses were carried out on 36 zircon grains. Only 28 analyses were considered valid, the rest being rejected because of either Pb loss (n = 4) or high common Pb content (>10 %; n = 4). Twenty-seven analyses yield a weighted mean age of 550 \pm 8 Ma, although with a high MSWD of 5. Notably, the range of crystallization ages is very broad, varying between 529 and 568 Ma. Different authors (e.g., Siégel et al., 2018; Dahlquist et al., 2024, and references therein) recommend using combined diagrams to discriminate age populations to identify zircon antecrysts and autocrysts. Combined linearized probability plots are shown in Fig. 3A and weighted mean age diagrams in Fig. 3B. Complete data used in these figures as well as further linearized probability plots are reported in Supplementary Material S5. These data allow us to distinguish three age populations, which are used here to calculate three consistent weighted mean ages (outside error limits) with low error and MSWD values: 532 \pm 6 Ma (MSWD = 0.08), 544 \pm 5 Ma (MSWD = 0.30), and 560 \pm 8 Ma (MSWD = 0.21). In addition, two individual ages of 573 and 574 Ma and four individual ages that yield 595 \pm 11 Ma (MSWD = 0.51) are also recognised (Fig. 3). These individual older ages cannot be discriminated



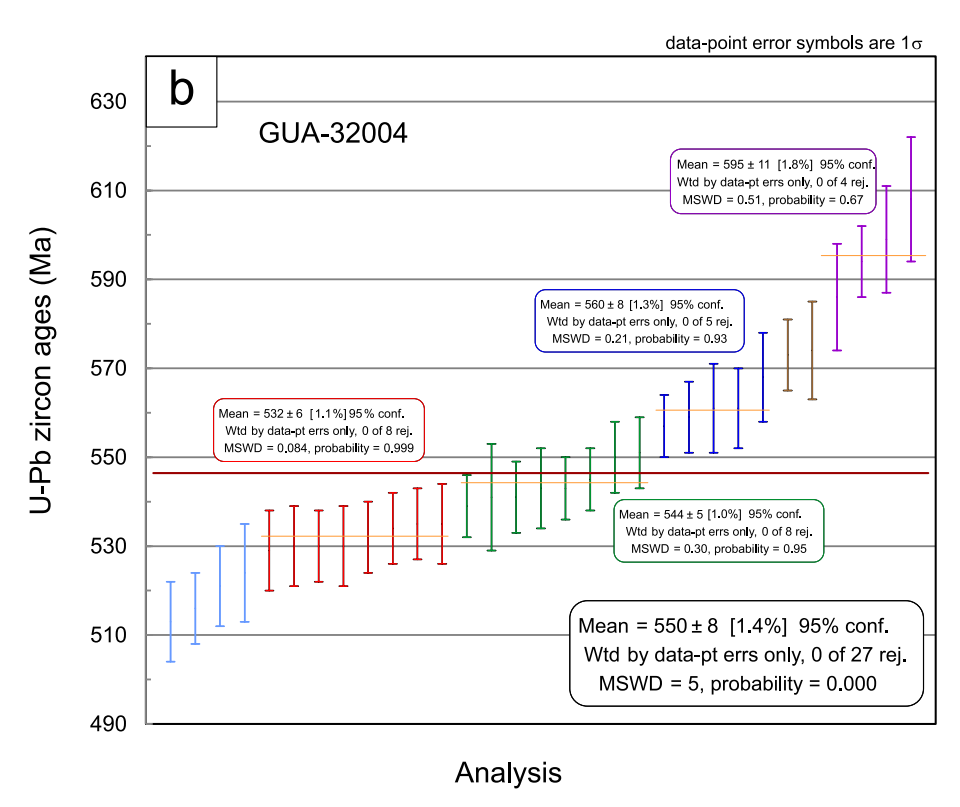


Fig. 3. A) Linearized probability plots using individual zircon U-Pb ages (n=27) from the analyses included in Supplementary Material S5. Taking the whole dataset, a regression line (brown line) with a relatively high error (\pm 50 Ma) for the calculated slope is obtained. By contrast, using the three age populations a lower error is obtained for the three calculated slopes (linearized probability plot discriminating populations age and individual weighted mean age are shown in Supplementary Material S5). Insets: 1) slope line regression and calculated age and 2) the weighted mean ages included in the figure are those shown in B). 3) Schematic multimodal distribution; where two inflection points (circle) in the curve fit line separate three component distributions (Rinehart et al., 2022). The numbers 1 and 2 indicate points of inflection between the fit lines defined by each population determined in this study. B) Weighted mean age plot showing the range of individual age values using the whole dataset from the sample GUA-32004 and the weighted mean age of the discriminated zircon populations. The four youngest ages, interpreted as affected by Pb loss (see text), were not used in the calculation. The inset shows the calculated age, albeit with a high MSWD value of 5.

using linearized probability plot, because a minimum of five data points is required. However, these individual ages are distinct from the group of 560 ± 8 Ma Ma (Fig. 3B).

The two youngest ages (i.e., 532 ± 6 and 544 ± 5 Ma) are taken as two major crystallization events during the magmatic activity of the Guasayán pluton, where the older age is interpreted as zircon antecrysts and the younger age may represent the emplacement age (i.e., zircon autocrysts). Based on detrital zircon ages (see below), ages ≥ 573 Ma are considered inherited zircon (i.e., xenocrysts), represented by two individual ages of 573 and 574 Ma, as well as an age of 595 ± 11 Ma, as described above. The age of 560 Ma can also be considered as inherited, according to the detrital zircon pattern of the Punconviscana Series (see discussion). A zircon grain of 658 ± 15 Ma is also interpreted as a xenocryst.

6.2. El Escondido pluton (GUA-32050)

A total of 36 analyses were carried out in 36 zircon grains. Only 26 analyses were considered valid because grains with Pb loss (n = 6) or high common Pb content (>10 %; n = 4) were discarded. A similar analysis to that conducted for the ages of the Guasayán pluton can be carried out for the El Escondido pluton. Notably, four weighted mean ages comparable to those of the Guasayán pluton can be identified on 23 analyses (sample 32050): 533 \pm 5 Ma (MSWD = 0.15), 546 \pm 3 Ma (MSWD = 0.76), 562 \pm 5 Ma (MSWD = 0.47) and 590 \pm 6 Ma (MSWD = 1.4) (Fig. 4). Similarly, the two older ages are considered as xenocrysts, whereas the two younger ages are interpreted as representing two major crystallization events during the magmatic activity of the El Escondido pluton. The age of 546 \pm 3 Ma would correspond to zircon antecrysts, and the youngest age is considered as the emplacement age (i.e., zircon autocrysts). Five concordant older ages of 607 \pm 9 Ma, 607 \pm 13 Ma, 616 \pm 9 Ma, 656 \pm 9 Ma and 1143 \pm 2 Ma were also identified as xenocrysts.

6.3. Alto Bello granodiorite (GUA-32023)

A total of 111 analyses were carried out in 96 zircon grains (17 grains with core and rim analyses). Only inherited zircon ages were obtained highlighting two main populations. A first population with most ages between 700 and 600 Ma (n = 24) and a second one with ages between 1200 and 900 Ma (n = 56). In addition, we can also discriminate another small group with ages between 900 and 700 Ma (n = 10). Some scarce ages between 2000 and 1800 Ma (n = 6) and 2900 and 2500 Ma (n = 3) are also present. The youngest zircon grain yielded an age of 572 \pm 6 Ma

6.4. Metapsammite country rock (GUA-23062)

A total of 57 analyses were carried out in 57 zircon grains. The oldest age is ca. 1200 Ma. The youngest age is 589 \pm 7 Ma. The age population is bimodal, with ages between 750 and 600 Ma (n = 18) (Neoproterozoic) and 1080 and 800 Ma (n = 23) (Mesoproterozoic to Neoproterozoic). There are also scarce Paleoproterozoic ages around 1900–1800 Ma (n = 5) and Neoarchean ages of 2700–2600 Ma (n = 4). This pattern is very similar to those reported for the Puncoviscana Series elsewhere (Escayola et al., 2007, 2011; Rapela et al., 2007, 2016; Adams et al., 2008; Hauser et al., 2011; Iannizzotto et al., 2013; Casquet et al., 2018). The absence of zircon grains with Paleoproterozoic ages between 2.26 and 2.02 Ga (Rapela et al., 2007) rules out the participation of the Rio de la Plata craton and other Paleoproterozoic cratons with these ages as potential sources of sediments.

7. Whole-rock chemistry

In this section the main geochemical characteristics of the granitoids from the Sierra de Guasayán are described together with those from the Pampean arc elsewhere (Figs. 6, 7 and 8; Supplementary Material S1 and S3).

The granitoids of the Guasayán complex are mainly intermediate to felsic rocks, very similar to those of the Pampean arc elsewhere. These rocks range in composition from diorite to syenogranite and their volcanic equivalents. They are subalkaline with most rocks showing SiO2 contents between 60 wt% and 74 wt%, and high-K compositions (Fig. 6). They are mainly magnesian and calc-alkalic (Fig. 6) with the most basic samples ($SiO_2 < 60$ wt%) showing calcic affinities, whereas subordinate alkali-calcic compositions are also present. The rocks with $SiO_2 \le 60$ wt % are clearly metaluminous with ASI (molar $Al_2O_3/CaO + Na_2O + K_2O$) ranging from 0.65 to 0.97 (Fig. 6E), also showing a positive correlation with SiO2, whereas most samples are slightly to moderately peraluminous with ASI varying between 0.95 and 1.2 (Fig. 6E). In addition, although less representative, strongly peraluminous compositions (ASI: 1.25–1.5) are also recorded in samples with SiO₂ higher than 64 wt%. These traits are also observable in the A-B diagram of Debon and Le Fort (1983), with most samples showing low to mildly peraluminous compositions, whereas highly peraluminous and metaluminous compositions are minor (Fig. 6F). The metaluminous compositions are mainly restricted to mafic enclaves and small-scale diorite to tonalite outcrops.

Harker diagrams (Fig. 7) show clear negative correlations of FeO, MgO, TiO_2 and CaO with SiO_2 , a positive correlation between K_2O and SiO_2 , as well as scattered but nearly constant values of Na_2O and Al_2O_3 , although it seems that the silica richer compositions have lower contents of Al_2O_3 than the most basic ones. No clear relations between P_2O_5 and SiO_2 are observable (Fig. 7).

The La Soledad quartz diorite from the Sierra de Guasayán has the highest TiO_2 content and most granitoids from the Sierra the Guasayán are also relatively enriched in TiO_2 .

Chondrite-normalized REE and Silicate Earth normalized traceelement patterns of the granitoids from the Sierra de Guasayán are very similar to those of the late Ediacaran to early Cambrian igneous rocks from the Sierras Pampeanas, North Patagonian Massif, Cordillera Oriental and Puna (Fig. 8). Chondrite-normalized REE patterns are enriched in LREE with respect to HREE ($La_N/Lu_N = 4.08-14.71$), mainly showing negative slopes with a variably marked negative Eu anomaly (Eu/Eu* = 0.35–0.86), although minor samples with positive Eu anomaly (Eu/Eu* = 1.03–1.06) are also present in the Guasayán pluton and other outcrops from the Sierras Pampeanas and Puna. A few basic samples from the Puna have lower LREE values resulting in flat patterns $(La_N/Lu_N = 1.53-1.80 \text{ and } Eu/Eu^* = 0.79-0.80; \text{ Fig. 8}). \text{ Silicate Earth}$ normalized trace-element patterns are enriched in incompatible elements showing troughs in Ba, Nb-Ta, Sr and Ti, a large spike in Pb (when measured), a small spike in Zr, and variable values of Th and P that result in positive and negative anomalies (Fig. 8).

8. Rb-Sr and Sm-Nd isotopes

Eight granitic samples from the Sierrra de Guasayán have been selected for Sr and Nd isotope analysis (Fig. 9; Supplementary Material S1 and S4): three from the main Guasayán pluton, three from the El Escondido pluton, one from the La Soledad quartz diorite and another from the El Martirizado pluton. These samples are studied along with other Cambrian arc-related rocks with published Sr and Nd isotope data (n = 24). In addition, a set of samples of the Puncoviscana Series and Cambrian S-type granites related to younger regional metamorphism with Sr and Nd data have also been compiled for comparison (full list is reported in the Supplementary Material S4).

Initial radiogenic isotope ratios were calculated at 530 Ma (time of the main activity of arc magmatism). Two-stage Nd model ages (T_{DM}) were calculated with respect to the depleted mantle according to DePaolo et al. (1991). The 147 Sm/ 144 Nd in the analysed and compiled samples are below the threshold value of 0.165, above which calculated model ages tend to be unreliable (Stern, 2002b).

The samples from the Sierra de Guasayán show εNd_i values between

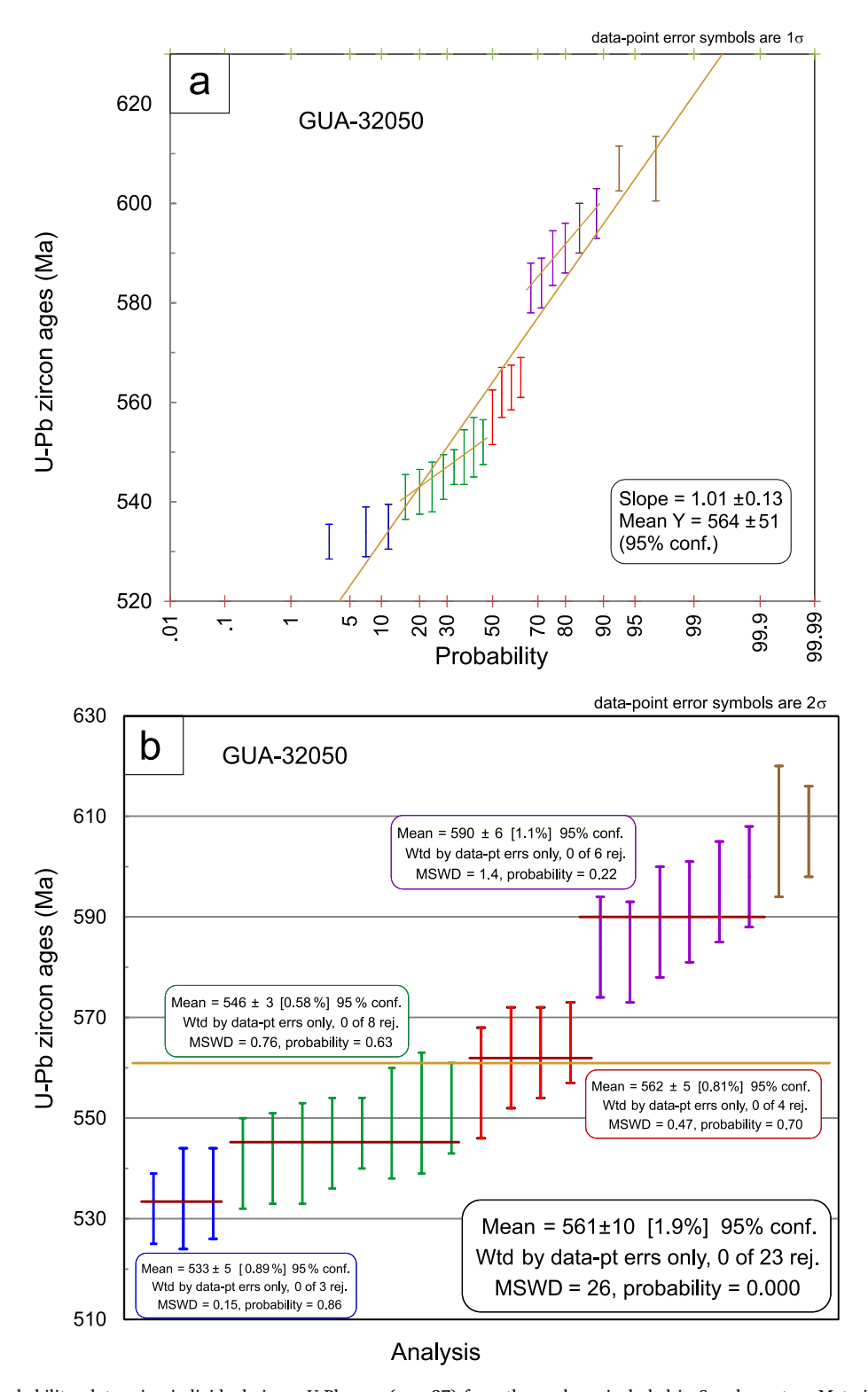


Fig. 4. A) Linearized probability plots using individual zircon U-Pb ages (n=27) from the analyses included in Supplementary Material S5. Taking the whole dataset, a regression line (brown line) with a relatively high error (\pm 50 Ma) for the calculated slope is obtained. By contrast, using the three age populations a lower error is obtained for the three calculated slopes (linearized probability plot discriminating populations age and individual weighted mean age are shown in Supplementary Material S5). Insets: 1) slope line regression and calculated age and 2) the weighted mean ages included in the figure are those shown in B). 3) Schematic multimodal distribution; where two inflection points (circle) in the curve fit line separate three component distributions (Rinehart et al., 2022). The numbers 1 and 2 indicate points of inflection between the fit lines defined by each population determined in this study. B) Weighted mean age plot showing the range of individual age values using the whole dataset from the sample GUA-32050 and the weighted mean age of the discriminated zircon populations. The inset shows the calculated age, which yields an age with a high MSWD value of 26.

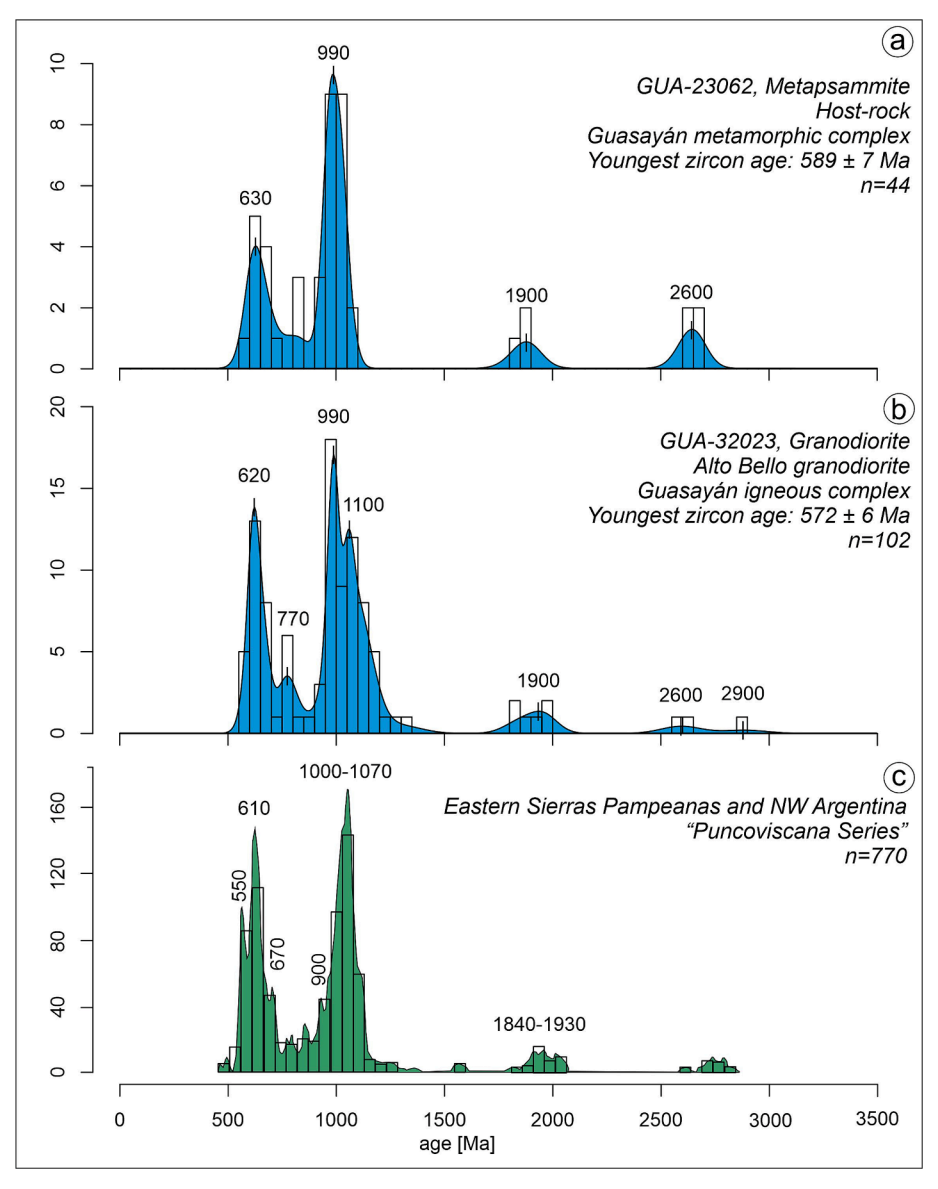


Fig. 5. Zircon probability density plots from sample GUA 32023 (Alto Bello granodiorite) and sample GUA 23062 (host-rock metapsammite). Probability plot of the Puncoviscana Series (Rapela et al. 2016) is included for comparison.

-2.4 and -4.2, along with Nd model ages that vary between 1.45 and 1.6 Ga (Fig. 9; Supplementary Material S1), and Sr/Sr_i between 0.70808 and 0.71207 (Fig. 9; Supplementary Material S1). These values match those of the other Pampean subduction-related granitoids with ϵNd_i mostly ranging from -0.5 to -5.9 and Sr/Sr_i between 0.70340 and 0.71494 (Fig. 9; Supplementary Material S1). There is only one diorite from the Puna with a positive εNd_i of + 1.8 and one granodiorite from the Tastil batholith with a more negative εNd_i of -9.8. The εNd_i values of most Pampean arc granitoids are within the range of the Puncoviscana Series (-3 to -7.7) with a few samples showing higher values (-2.6 to +1.8), whereas most samples show higher ϵNd_i than the Cambrian anatectic (S-type) granites (-4.8 to -6.5) linked to the regional metamorphism although with some overlap (Fig. 9). It should be noted that the Sr/Sr_i data of the Pampean arc-related granitoids (0.703-0.715) are in general less radiogenic than those of the Puncoviscana Series and the non-arc-related S-type granites (0.711–0.718).

9. Discussion

9.1. Meaning of antecrysts and the youngest zircon ages

Zircon antecrysts can be defined as grains crystallized in early magma stages or pulses that are later incorporated to new pulses (c.f., Miller et al., 2007). These antecrysts may originate from recycled material of older, solidified, or partially solidified intrusions, or they may result from the remobilization and mixing within a long-lived crystalline mush formed by previous intrusive events in a large reservoir at mid-to upper-crustal levels (Miller et al., 2007). Alternatively, they may indicate the presence of a long-lived deep magmatic reservoir where antecrysts incubate, while autocrysts crystallize during emplacement at shallower crustal levels (e.g., Cashman et al., 2017; Lim et al., 2023; Dahlquist et al., 2024; Santos da Cruz et al., 2024).

The presence and implications of antecrysts within the context of the Pampean magmatic arc have not been previously reported or considered. Published ages of Pampean granitoids typically peak around 540–520 Ma (ca. 530 Ma; see review by Casquet et al., 2018), with even younger ages reported for the Puna igneous complexes (520–505 Ma;

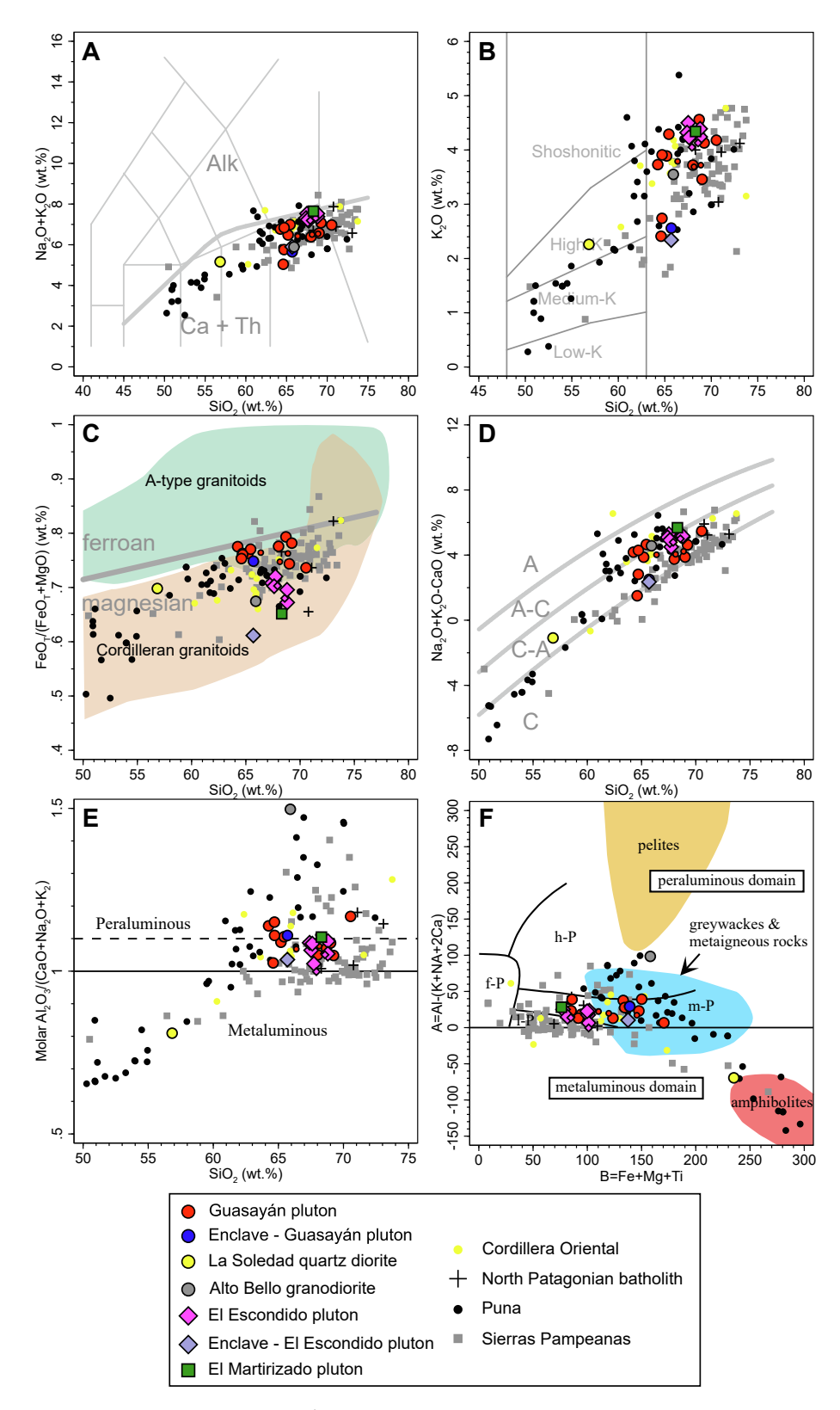
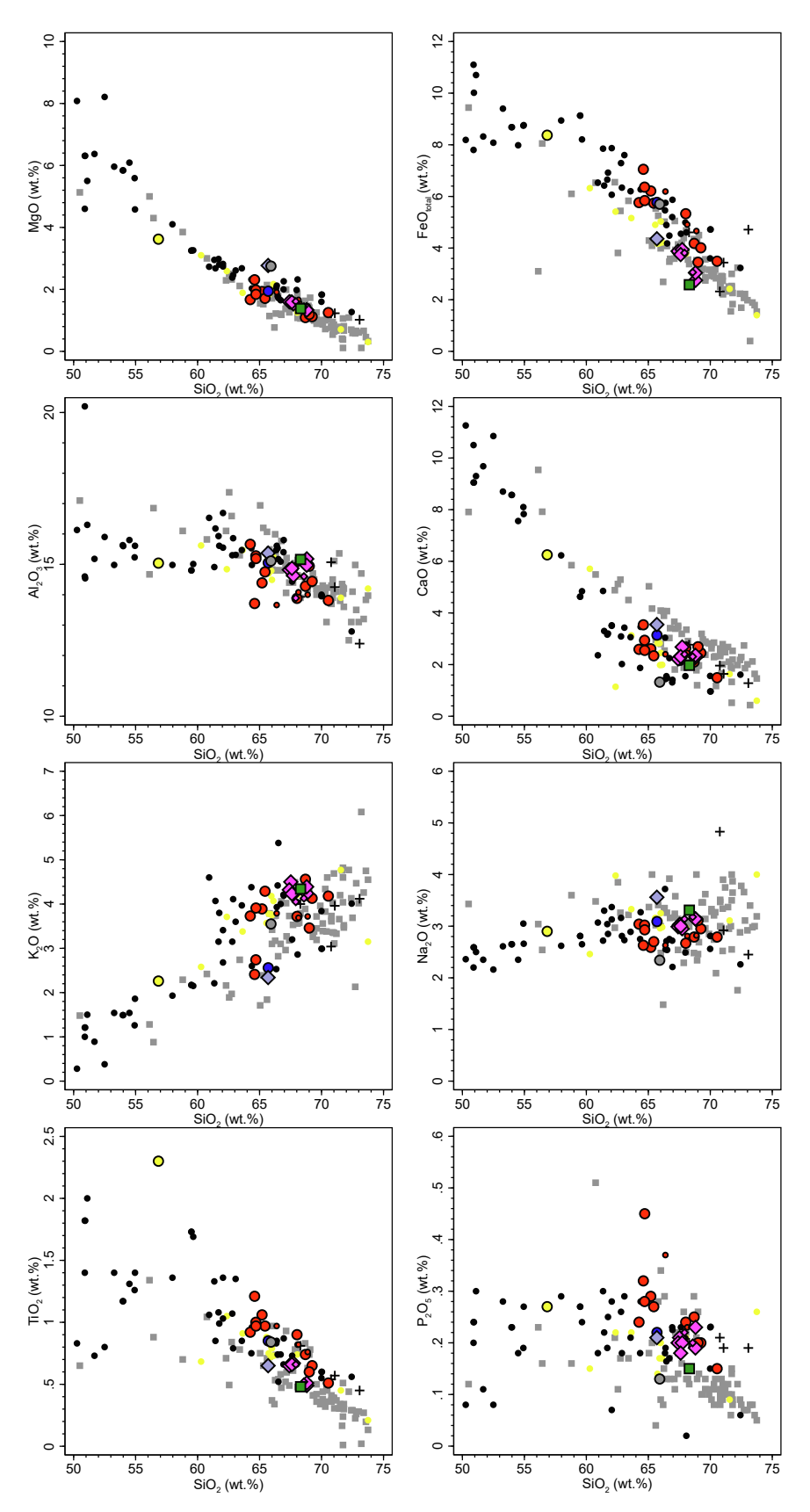


Fig. 6. Whole-rock composition of the granitoids from the Guasayán complex and the rest of the Pampean arc granitoids. A) Total alkalis vs. silica (TAS) diagram. B) SiO₂ v. K₂O diagram. C) Fe-number vs. SiO₂ diagram. A-type and Cordilleran granitoid fields after Frost et al. (2001). D) MALI-index vs. SiO₂ diagram after Frost et al. (2001). E) Molar alumina saturation index vs. SiO₂. F) A-B diagram after Debon and Le Fort (1983), modified by Villaseca et al. (1998). Small red squares and magenta diamonds represent data from the Guasayán and El Escodio plutons taken from Bellos et al. (2020a). (For interpretation of the references to colour in this figure legend, the reader is referred to the web version of this article.)



 $\textbf{Fig. 7.} \ \ \textbf{Harker diagrams for the Pampean arc granitoids. Symbols as in Fig. 6.}$

Gondwana Research 150 (2026) 228-253

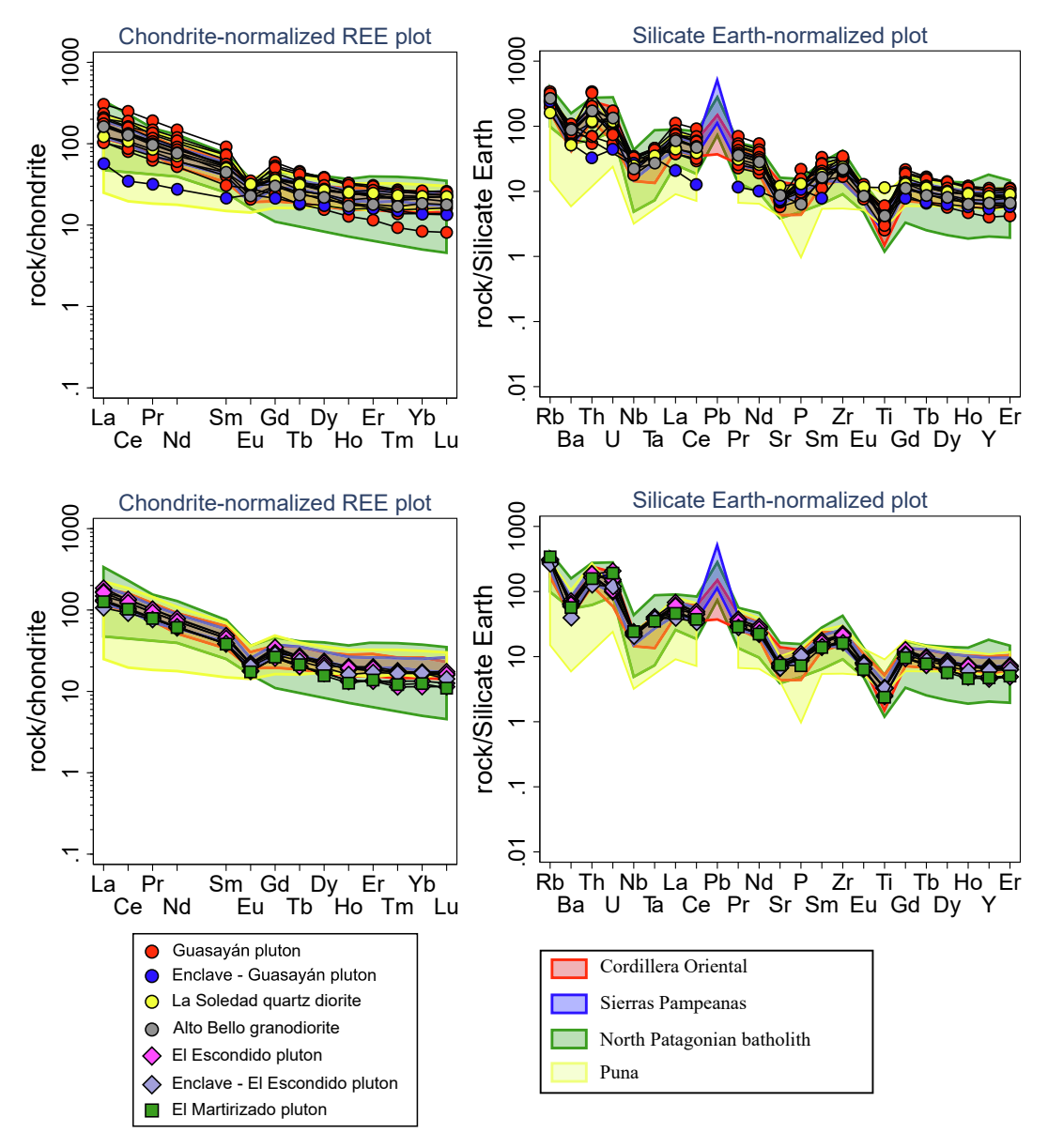


Fig. 8. Chondrite-normalized REE and Silicate Earth-normalized trace element diagrams. Normalization values after McDonough and Sun (1995). Compositional fields of arc-related granitoids from Puna, Cordillera Oriental, Sierras Pampeanas and the North Patagonian batholith are shown for comparison.

Ortiz et al., 2017, 2019; Suzaño et al., 2017), although these later may be questionable as discussed below. However, it is important to note that this age range reflects crystallization ages of several distinct igneous units. Interestingly, the age range of ca. 545–525 Ma is fully represented among the antecrysts and autocrysts of the studied samples from the Guasayán complex, indicating a unique long-lasting magmatic system previously unrecognised.

Interestingly, scarce zircon grains with ages of 555–540 Ma that match those of the antecrysts in the Guasayán granitoids, have also been reported from intrusions elsewhere, i.e., the Tastil and Sierra Norte-Ambargasta batholiths (Hauser et al., 2011; Iannizzotto et al., 2013), the Tardugno granodiorite (Rapalini et al., 2013; Pankhurst et al., 2014), the Guasayán pluton (Dahlquist et al., 2016), the Pachamama complex (Ortiz et al., 2019) and the Pabellón granodiorite (Bellos et al., 2020b). However, these ages have been integrated into the overall age calculations for these rocks (Hauser et al., 2011; Iannizzotto et al., 2013; Rapalini et al., 2013; Dahlquist et al., 2016), blurring them within the statistics of the younger dominant ages, or being interpreted as inherited zircon ages (Pankhurst et al., 2014; Ortiz et al., 2019; Bellos et al., 2020b). Similarly, a broad range of ages from ca. 560 to ca. 520 Ma was

recorded in individual S-type granite samples from the Saldania orogen (Villaros et al., 2012), but these ages were collectively used to estimate a crystallization age.

Therefore, the occurrence of zircon antecrysts (ca. 545 Ma) may be extended to other igneous bodies of the Pampean-Saldania arc, suggesting the existence of long-lived magmatic systems within this region. Recently, such long-lasting magmatic systems have also been documented in several igneous complexes developed in different geodynamic settings (e.g., Lim et al., 2023; Dahlquist et al., 2024; Santos da Cruz et al., 2024). However, specifying the mechanisms responsible for generating antecrysts is beyond the scope of this work.

The younger ages reported for Cambrian granitoids in the Puna could indicate a diachronous development of magmatism in the Pampean arc with generation of younger granites to the North. However, it could also be due to misleading interpretations of the data, since the youngest ages (ca. 520 Ma or younger, as suggested in this work) could result from Pb loss triggered by younger thermal events, such as the regional metamorphism and anatectic peraluminous granitic magmatism developed at ca. 527–520 Ma (e.g., Rapela et al., 1998; Murra et al., 2016; Larrovere et al., 2021, and references therein), the Famatinian magmatism

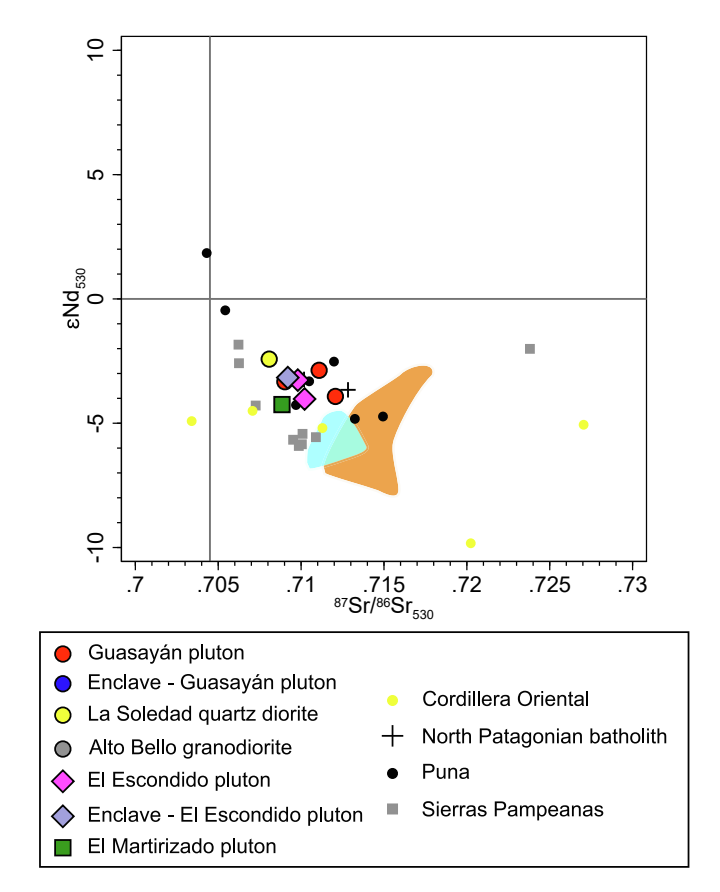


Fig. 9. ϵ Nd_i vs. Sr/Sr_i diagram. Compositions of younger Cambrian S-type granites (light blue field; data from Rapela et al., 1998) and metasedimentary rocks of the Puncoviscana Series (orange field; data from Rapela et al., 2002) are shown for comparison. (For interpretation of the references to colour in this figure legend, the reader is referred to the web version of this article.)

(490–460 Ma; Rapela et al., 1998, 2018; Weinberg et al., 2018; Otamendi et al., 2020) or the Silurian Rinconada tectono-thermal event (445–410 Ma; Casquet et al., 2021). In the present study, zircon grains with ages younger than ca. 520 Ma (524–513 Ma; n = 9) have been considered as affected by loss of radiogenic Pb. It is worth noting that proportionally minor or scarce ages, younger than ca. 520 Ma (range: 520–500 Ma), have been commonly reported and indistinctively included or excluded in the age calculation of several Pampean arc granitoids (e.g., Hauser et al., 2011; Iannizzotto et al., 2013; Rapalini et al., 2013; Pankhurst et al., 2014; Bellos et al., 2020b).

9.2. Crystallization ages of granitoids from Guasayán intrusive complex and the other Pampean arc plutons

Cambrian ages for granitic rocks from the Sierra de Guasayán were first obtained by K-Ar in biotite. Thus, González and Toselli (1974) reported an age of 541 ± 7 Ma for rocks from the east flank of the Sierra de Guasayán. Omil (1992) obtained ages of 500 ± 20 Ma, 506 ± 14 , 515 ± 15 and 519 ± 20 Ma in samples from the Guasayán Pluton collected close to Villa Guasayán. By contrast, Dal Molin et al. (2003) reported controversial younger ages for samples from the Guasayán (380 \pm 20) and El Escondido plutons (425 \pm 21 Ma).

A crystallization U-Pb zircon age (LA-MC-ICP-MS) was obtained by Dahlquist et al. (2016), reporting an age of 533 ± 4 Ma for a biotite granodiorite (GUA-1) from the Guasayán pluton, which is close to the K-Ar age reported by González and Toselli (1974).

Although a crystallization age for the Alto Bello granodiorite could not be obtained (see next section), the two new U-Pb zircon ages of the Guasayán and El Escondido plutons corroborate the inferred Cambrian age (González and Toselli, 1974; Dahlquist et al., 2016). Samples GUA 32004 (532 \pm 6 Ma, Guasayán pluton) and GUA 32050 (533 \pm 7 Ma, El Escondido pluton), are roughly coeval with ages similar to that obtained by Dahlquist et al. (2016). These ages imply that the Cambrian granites from the Sierra de Guasayán were formed during the flare-up of Pampean arc magmatism at 530–535 Ma (Casquet et al., 2018).

Furthermore, considering the ages of the antecrysts and autocrysts (ca. 545 Ma and ca. 530 Ma), the Guasayán intrusive complex shares a significant portion of the magmatic activity regionally recorded in the Pampean arc. These ages are similar to the U-Pb zircon ages reported for the Sierra Norte-Ambargasta batholith (540-530 Ma, Schwartz et al., 2008, TIMS; Siegesmund et al., 2010, SHRIMP; Iannizzotto et al., 2013, SHRIMP; Von Gosen et al., 2014, SHRIMP), granitoids from Cumbres Calchaquíes (522 Ma, Bellos et al., 2020b, SHRIMP), Tastil batholith and other outcrops in the Cordillera Oriental (540-525 Ma, Hongn et al., 2010, TIMS; Aparicio González et al., 2011, LA-MC-ICP-MS; Hauser et al., 2011, LA-MC-ICP-MS), igneous complexes from the Puna (520-505 Ma, LA-MC-ICP-MS; Ortiz et al., 2017, 2019; Suzaño et al., 2017, and references therein). Rapalini et al. (2013; SHRIMP) and Pankhurst et al. (2014; SHRIMP) also reported Cambrian granitoids with U-Pb zircon ages around 530-520 Ma from the North Patagonian massif, suggesting the extension and continuity of the arc magmatism to the south of Río Colorado. Chernicoff et al. (2012) also reported SHRIMP U-Pb zircon ages of 528 \pm 5 Ma and 520 \pm 1.4 Ma (El Carancho complex) for metaigneous rocks from La Pampa province that could represent part of the magmatic arc. However, the Th/U values of those zircon grains is low and may indicate metamorphic processes as the authors mentioned, then it is not clear whether they represent crystallization ages or not. Several ages older than 540 Ma have also been reported (Söllner et al. 1991; Llambías et al. 2003; Schwartz et al., 2008), but they have not been considered here because of the reliability of the data, considering for instance the complexity of the zircon grains and the method (e.g., TIMS), as discussed by Baldo et al. (2014).

Recently, the Pampean orogeny and the Saldania orogenic belt in South Africa have been correlated and integrated as part of the same active continental margin in southwestern Gondwana (Casquet et al., 2018). The Saldania Belt is characterized by voluminous S-type and minor I-type (syn- to late-tectonic) and A-type (post-tectonic) granites of the Cape Granite Suite, emplaced into the Malmesbury Group in the southern and western Saldania Belt, a sedimentary formation equivalent to the Puncoviscana Series (Belcher, 2003; Gresse et al., 2006; Farina et al., 2012; Frimmel et al., 2013; Kisters and Belcher, 2018). U-Pb zircon ages indicate the emplacement of the granites between approximately 550 and 510 Ma, with a peak of plutonic activity between ca. 540 and 530 Ma (Schoch, 1975; Scheepers, 1995; Da Silva et al., 2000; Scheepers and Schoch, 2006; Villaros et al., 2009; Chemale et al., 2011; Farina et al., 2012), an age-range that is very similar to the recorded in the Gusayán Intrusive Complex.

9.3. Zircon provenance and inheritance

9.3.1. Detrital zircon in the country rock of the Guasayán intrusive complex. A metapsammite from the Guasayán complex, which serves as the host rock for the Guasayán granitoids, shows a marked resemblance to the Puncoviscana Series, particularly in the detrital U-Pb zircon age distribution. The zircon age patterns in the Puncoviscana Series are bimodal, with prominent peaks at 1100–960 Ma and 680–570 Ma, and minor populations at 2000–1700 Ma and around 2600 Ma (Rapela et al., 2007, 2016; Adams et al., 2008; Hauser et al., 2011). Fig. 5 presents a comparative analysis of the zircon age patterns from the Guasayán metapsammite and the Puncoviscana Series.

Both age spectra feature two main principal groups: one ranging from 690 to 560 Ma and a Grenvillian group between 960 and 1100 Ma. Notably, there is an absence of zircon grains corresponding to the Rio de la Plata Craton, which is typically dated between 2.02 and 2.26 Ga (Rapela et al., 2007). These findings suggest that the Guasayán

metamorphic basement was part of the broader Ediacaran Puncoviscana Saldanian basin (Casquet et al., 2018) in SW Gondwana.

9.3.2. Zircon inheritance in the Pampean arc granitoids

A common feature of the studied granites from the Sierra de Guasayán is the presence of inherited zircon grains (Dahlquist et al., 2016; this study), especially important in the Alto Bello Granodiorite, in which no crystallization age could be determined. This may be attributed to the strongly peraluminous nature of this magmatic unit. In magmas with such a strongly peraluminous composition the dissolution of zircon and precipitation of new zircon during crystallization/ emplacement can be hindered or restricted to small tips or rims hard to date (Watson and Harrison, 1983; Watson, 1996; Farina et al., 2014; Morales Cámera et al., 2017), preventing the determination of the crystallization age. The inherited zircon age pattern in the Alto Bello Granodiorite closely resembles that of the Guasayán metapsammite (Fig. 5), exhibiting a bimodal distribution with two main Proterozoic age groups (750-600 Ma and 1200-800 Ma) and minor Paleoproterozoic ages. This suggests that the peraluminous magmatism associated to the Pampean arc was primarily sourced from the Puncoviscana Series. Similarly, the peraluminous granitoids of the South African Saldania orogen, roughly coeval with the granitoids of the Guasayán complex, show a U-Pb inherited zircon age pattern resembling the Saldanian metasedimentary Malmesbury Formation, which is the equivalent of the Puncoviscana Series (Villaros et al., 2012; Casquet et al., 2018). Thus, the crustal component of the S-type magmas was probably derived from the Puncoviscana - Saldanian sedimentary basin.

This feature is also observed in the dominant Cambrian units of the Pampean arc, which, although peraluminous or metaluminous, also display zircon inheritance. Neoproterozoic ages are by far the most common in the studied samples from the Guasayán and El Escondido plutons, with two important populations at ca. 590 and 560 Ma, and single ages of 658 Ma and 656 Ma. In addition, a Grenvillian age of 1143 \pm 18 Ma has been recognised in the sample from the El Escondido pluton. These ages are broadly consistent with those reported by Dahlquist et al. (2016) for the Guasayán pluton (966 and 616 Ma).

Interestingly, similar groups of inherited zircon ages: 580–560 Ma, 630–600 Ma, and 1300–900 Ma, have also been reported from Pampean arc granitoids from the Puna and Cordillera Oriental, Sierra Norte-Ambargasta batholith and North Patagonian Massif (Hauser et al., 2011; Iannizzotto et al., 2013; Pankhurst et al. 2014; Ortiz et al., 2017; Ortiz et al., 2019). Again, these groups of zircon ages are coincident with those of the Puncoviscana Series (Rapela et al., 2007, 2016; Escayola et al., 2007, 2011; Adams et al., 2008; Hauser et al., 2011; Iannizzotto et al., 2013, Casquet et al., 2018; this study), underscoring the significant role of the Puncoviscana Series not only as the basement where the Pampean arc granites intruded, but also as the primary source of the crustal component of the Pampean arc granitoids.

9.4. Characterization and classification of the Pampean arc granitoids

As formerly stated, several intermediate to felsic plutons and volcanic rocks in the Puna, Cordillera Oriental, Sierras Pampeanas and North Patagonian Massif form the Pampean arc. In spite of significant geochemical and mineralogical differences, they show similar patterns and evolutionary trends. They are essentially subalkaline and magnesian but with variable compositions that range from calcic to alcali-calcic and from metaluminous to strongly peraluminous. Nevertheless, its classification is not straightforward, although most of them are calc-alkalic and peraluminous, with some of them showing clear mineralogical and geochemical characteristics of I-type granitoids and other of S-type granitoids.

The least evolved rocks, represented by widespread small outcrops and enclaves of diorite to tonalite composition (SiO_2 range: 50.5 - 62.9 wt%), are clearly metaluminous, magnesian, mostly calcic and mediumto high-K (Fig. 6). Their distinctive mineralogy is represented by biotite

and amphibole with common occurrence of titanite and/or epidote, as well as apatite, zircon and opaque minerals as accessories (Lira et al., 1997; 2014; Ortiz et al., 2017; Suzaño et al., 2017; Zandomeni et al., 2021). Accordingly, both the mineralogy and geochemistry point to a calc-alkaline I-type affinity for this group of rocks.

Very minor felsic ($SiO_2 > 65$ wt%) and strongly peraluminous ($ASI \ge 1.25$), mainly magnesian and alcali-calcic compositions are also recognised as pertaining to the arc (Fig. 6) in the Puna, Cordillera Oriental and Sierras Pampeanas (Aparicio González et al., 2011; Suzaño et al., 2015, 2017; Ortiz et al., 2017; Bellos et al., 2020b), with the Alto Bello granodiorite in the Guasayán complex being the most peraluminous case (ASI = 1.5). The highly peraluminous character of the Alto Bello granodiorite is reflected in the mineral composition that comprises muscovite, cordierite and sillimanite, with monazite, zircon, apatite, ilmenite, and rutile as accessory minerals (Zandomeni et al., 2021), whereas the other samples correspond to biotite-muscovite granodiorites to monzogranites with accessory rutile, apatite, zircon and opaque minerals (Suzaño et al., 2015, 2017; Ortiz et al., 2017; Bellos et al., 2020b). Therefore, these rocks may be considered S-type granites.

However, the most abundant rocks of the Pampean magmatic arc are granodiorites and lesser monzogranites with mostly magnesian, calcalkalic and slightly peraluminous compositions (Fig. 6). They are characterised by the variable presence of minerals that are typical or distinctive of either I-type (e.g., amphibole, titanite, epidote, allanite) or S-type (e.g., muscovite, garnet, rutile, monazite) granites (e.g., Iannizzotto et al., 2013; Lira et al., 2014; Suzaño et al., 2015, 2017; Ortiz et al., 2017; Zandomeni et al., 2021). Amphibole has been only recognised in granodiorites and to a lesser extent in monzogranites from the Sierra Norte Ambargasta batholith (Lira et al., 1997, 2014), which could be classified as calc-alkaline I-type granites. Nonetheless, the variable presence of these chemically contrasting minerals (e.g., muscovite + titanite \pm epidote) in most of the rocks representing this magmatism, points to a hybrid nature for these rocks, which was previously envisaged from textural evidence and field relations (e.g., rapakivi texture, mafic enclaves, plagioclase zoning), mineral chemistry (mainly biotite compositions), whole-rock geochemistry and isotopes (Suzaño et al., 2015, 2017; Lira et al., 2014; Ortiz et al., 2017; Bellos et al., 2020a, 2020b, 2024; Zandomeni et al. 2021). In addition, the relatively low U and Th contents in the zircons of the studied samples may reflects a Stype affinity. Therefore, the voluminous granodiorites and monzogranites of the Pampean magmatic arc may be better classified as hybrid or transitional I-S-type granitoids as proposed by Zandomeni et al. (2021) for the Guasayán complex, although some of the Sierra Norte-Ambargasta granitoids (with ± amphibole) may represent less hybridized and/or more I-type like rocks within these overall I-S-type granitoids.

The different groups of arc rocks are well portrayed in the multicationic A-B diagram of Debon and Le Fort (1983; modified by Villaseca et al., 1998) (Fig. 6F). In this diagram, most samples plot as low to mildly peraluminous rocks following a roughly subhorizontal trend (Fig. 6F), similar to that reported by Grosse et al. (2011) for younger transitional I-S-type Ordovician (Famatinian) granitoids of the Sierra de Velasco. This trend is not typical of either I-type or S-type granites (Villaseca et al., 1998). Remarkably, the Sierra Norte-Ambargasta granitoids show a roughly negative trend from metaluminous to low peraluminous compositions that is consistent with their less hybridized character. On the other hand, samples that plot as either strongly peraluminous or metaluminous (with a negative trend) (Fig. 6F), correspond to those classified as true S-type and I-type granitoids respectively, based on mineralogical and whole-rock major elements compositions.

In the P_2O_5 vs SiO_2 plot (Fig. 7), we observe that for $SiO_2 > 60$ wt%, most samples from the Sierra Norte–Ambargasta batholith (the largest subset of the Sierras Pampeanas data) show a negative trend—albeit with some scatter—typical of I-type granites (Chappell, 1999; Chappell and White, 2001). In contrast, the remaining Pampean arc samples are more scattered and display higher P_2O_5 contents, suggesting a stronger

S-type affinity. In addition, in the CaO vs. FeO and Na_2O vs K_2O diagrams, the most mafic rocks besides many samples from the Sierra Norte Ambargasta batholith plot as I-type granites, whereas all rocks from the Guasyán complex and most of the Pampean arc granitoids show greater S-type character plotting in the overlapping area of I-type and S-type granites (Fig. 10).

Summarizing, the Pampean arc granitoids are represented by diorites to quartz diorites with a clear calc-alkaline I-type affinity, strongly peraluminous granites with an evident S-type signature and the most voluminous granodiorites, such as those of the Guasayán intrusive complex, with hybrid characteristics between I- and S-type granites. It should be noted that within this later group, granitoids from the Sierra Norte Ambargasta batholith show the strongest I-type affinity, likely representing the least hybridized rocks within the group.

9.5. Geochemical and isotopic constraints on magma sources

The hybrid or transitional nature of most of the rocks generated in the Pampean arc makes it necessary to constrain the likely involved sources, as a first step to better understand the petrogenetic mechanisms that gave rise to such magmatism. For that, we examined first the wholerock major and trace element compositions and then the isotopic (whole-rock Sr and Nd, zircon Hf) compositions of the Pampean arc granitoids.

As stated by Villaseca et al. (1998), the peraluminousity of the melts may be ultimately determined by the source rock compositions. According to this, the metaluminous diorite to tonalite enclaves and small bodies (e.g., La Soledad quartz diorite), along with the amphibole biotite granodiorites from the Sierra Norte Ambargasta batholith should derive from a mafic igneous or metabasic source (Fig. 6F; Villaseca et al, 1998), whereas the S-type granitoids would come from metapelitic or metagreywacke sources and the most representative hybrid rocks of the

Pampean arc from any combination of crustal sources (Fig. 6F; Villaseca et al., 1998) and/or a mantle source (Chapman et al., 2021).

Comparing major element compositions of the Pampean arc granitoids with experimental melts in diagrams from Patiño Douce (1999), it seems clear that the Pampean granitoids are richer in Ca, Fe, Mg and Ti than pure metasedimentary melts (Fig. 11), mostly plotting within the field of amphibolite-derived melts. Consequently, a mafic component must be involved in the generation of these granitoids, which is also supported by the presence of mafic enclaves (e.g., Lira et al., 1997, 2014; Ortiz et al., 2017; Suzaño et al., 2017; Zandomeni et al., 2021) that in most cases have amphibole (mainly hornblende and pargasite) as the main mafic mineral. Furthermore, most samples mimic the mixing lines between strongly peraluminous magmas and basaltic magmas modeled by Patiño Douce (1999) (Fig. 11), supporting their hybrid origin via the interaction of a mafic source and a felsic peraluminous component.

In the ternary source discrimination diagram of Laurent et al. (2014), most samples plot on the field of high-K mafic rocks and follow a clear trend from the 3 CaO apex toward the 5 K_2O/Na_2O apex with some samples plotting in the field of metasedimentary sources (Fig. 12). This trend indicates a continuous variation or interaction between mafic and metasedimentary sources, with the least evolved rocks (e.g., La Soledad quartz diorite) showing the highest affinity with the mafic source and the strongly peraluminous granitoids such as the Alto Bello granodiorite showing the highest affinity with the metasedimentary source. In addition, many samples like those from the Guasayán and El Escondido plutons straddle the boundary between the K-rich mafic sources and the metasedimentary sources with samples plotting in one field or the other indistinctly, strongly suggesting a hybrid origin.

Trace element ratios such as Ba/La, Cs/Sc and Zr/Yb can be used to track magma sources. Thus, LILE/HFSE ratios (e.g., Ba/La) are effective discriminators between fluid and sediment input in arc settings (e.g., Hawkesworth et al., 1993; Gamble et al., 1997), whereas Zr/Yb and Cs/

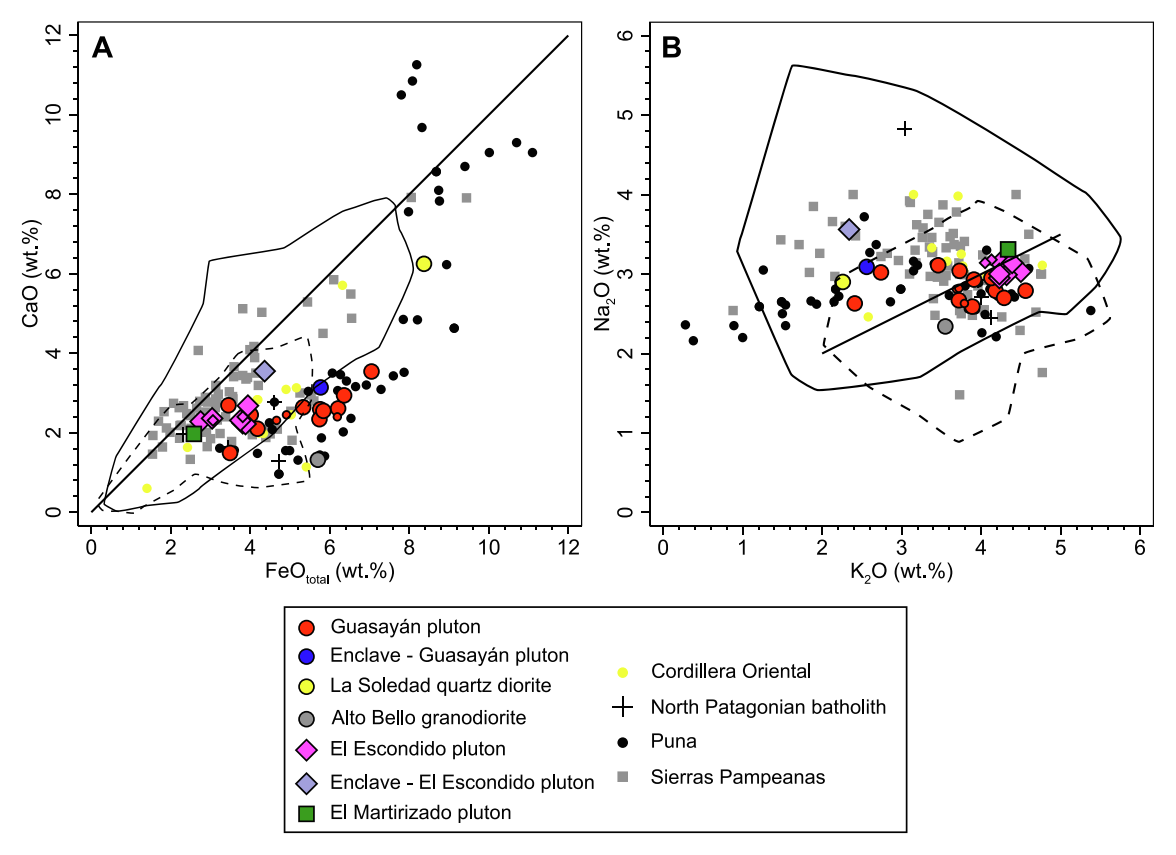


Fig. 10. A) CaO vs. FeO and B) Na_2O vs. K_2O relationships in the Pampean arc granitoids. Compositional fields after Chappell and White (2001). The black line in A) indicates 1:1 proportion. The line shown in B) joins the points 2% K_2O , 2% Na_2O and 5% K_2O , 3.5% Na_2O , originally given by Chappell and White (1974) as the boundary between I- and S-type granitoids.

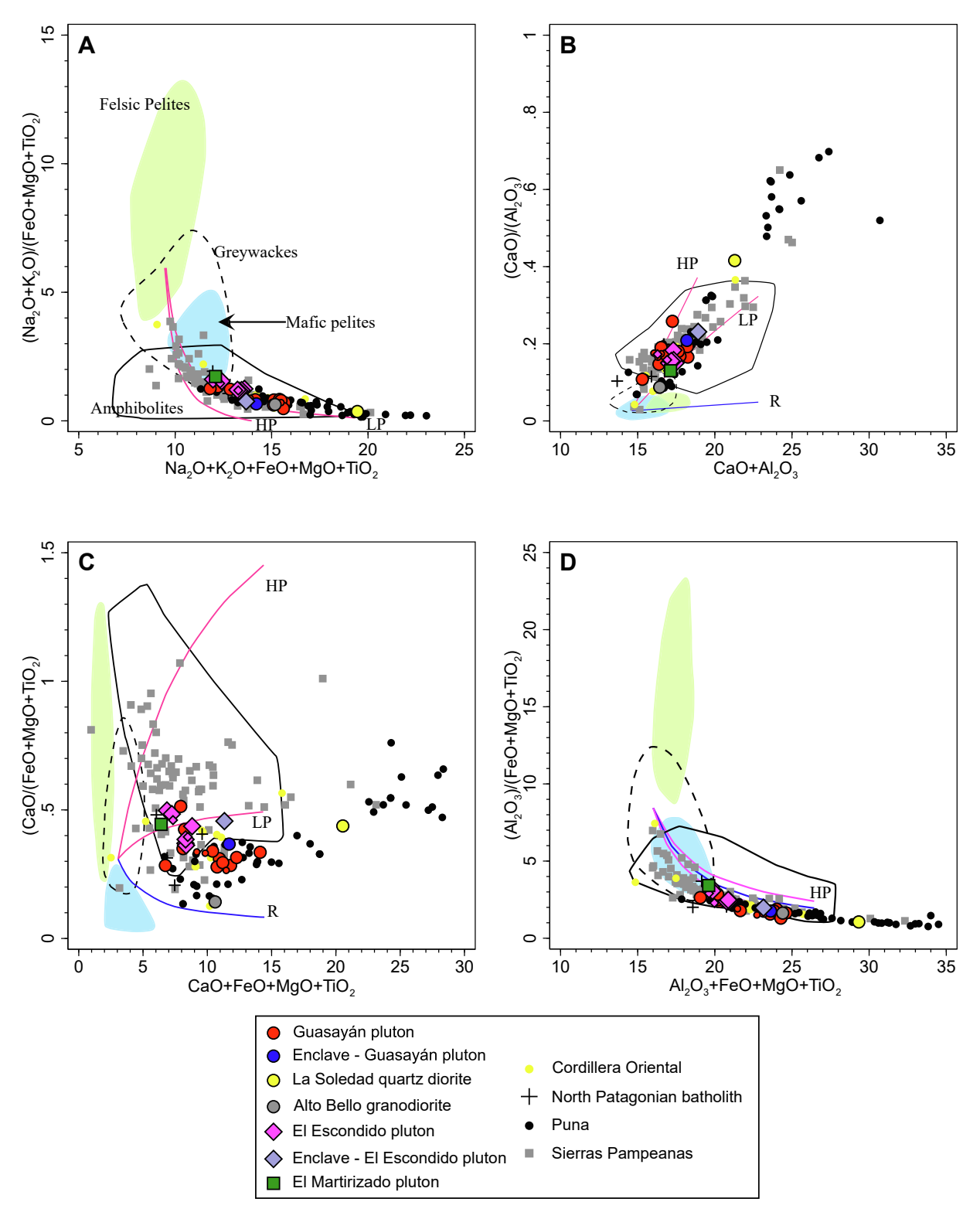


Fig. 11. A) $(Na_2O + K_2O)/(FeO + MgO + TiO_2)$ vs. $Na_2O + K_2O + FeO + MgO + TiO_2$. B) CaO/Al_2O_3 vs. $CaO + Al_2O_3$. C) $CaO/(FeO + MgO + TiO_2)$ vs. $CaO + FeO + MgO + TiO_2$. D) $CaO/(FeO + MgO + TiO_2)$ vs. $CaO + FeO + MgO + TiO_2$. D) $CaO/(FeO + MgO + TiO_2)$ vs. $CaO + FeO + MgO + TiO_2$. Compositional fields after Patiño Douce (1999). Pink lines represent hybridization trends between tholeitic basalt and metapelites modeled by Patiño Douce (1999) at low pressure (LP) and high pressure (HP) conditions. Blue line labeled R represents melt-restite mixing in a metapelitic system with no basaltic component (Patiño Douce, 1999). (For interpretation of the references to colour in this figure legend, the reader is referred to the web version of this article.)

Sc are good tracers of sediment involvement (Gamble et al., 1997). The Pampean arc granitoids have variable but relatively low Ba/La with most samples showing values close to the Primitive Mantle (10.2; McDonough and Sun, 1995), and high Cs/Sc and Zr/Yb ratios that in an

arc setting are indicative of a sedimentary source (Fig. 12; e.g., Gamble et al., 1997), giving also support to the hybrid nature of the Pampean arc granitoids.

The whole-rock isotopic Nd and Sr compositions of the diorites to

Gondwana Research 150 (2026) 228–253

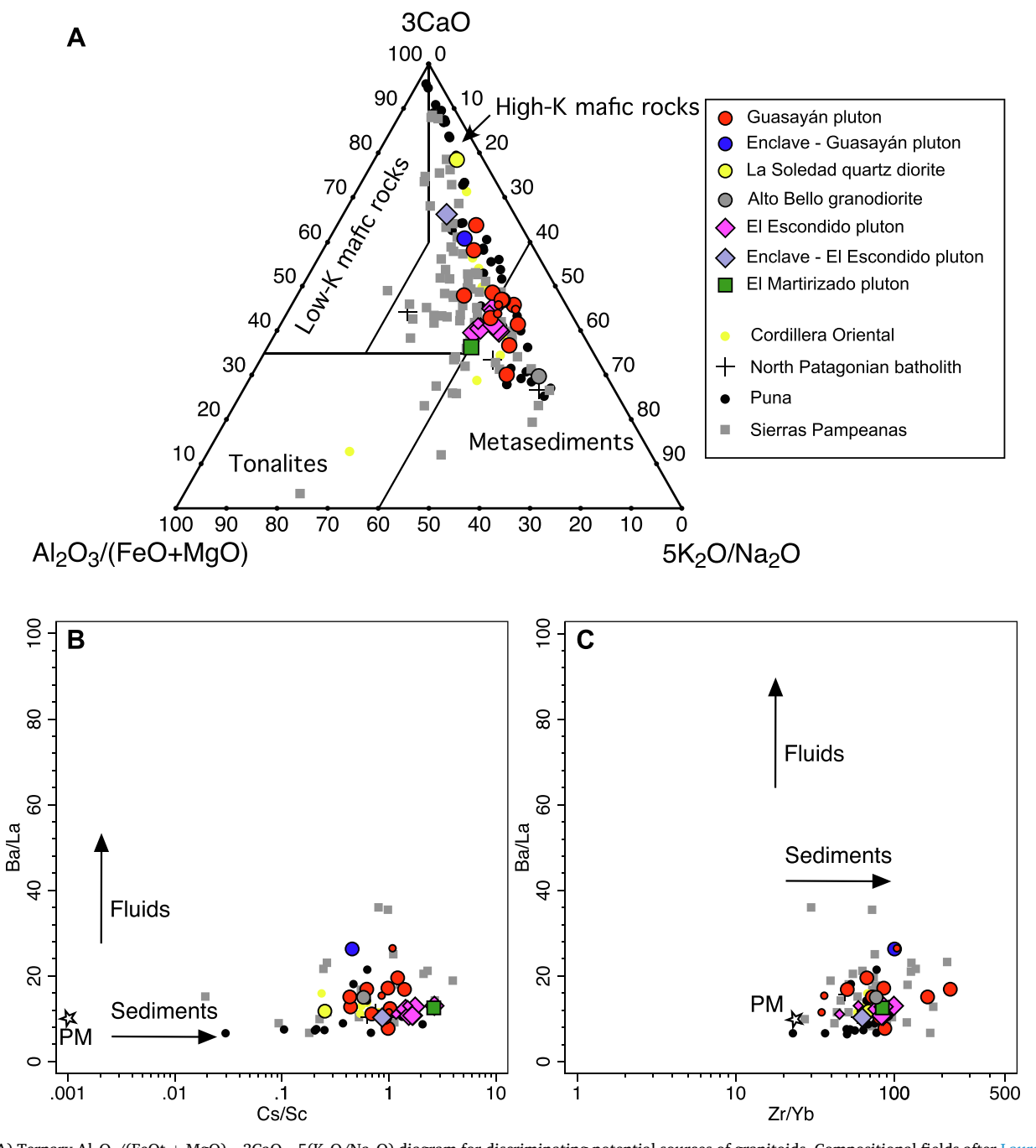


Fig. 12. A) Ternary $Al_2O_3/(FeOt + MgO) - 3CaO - 5(K_2O/Na_2O)$ diagram for discriminating potential sources of granitoids. Compositional fields after Laurent et al. (2014). B) Ba/La vs. Cs/Sc and C) Ba/La vs. Zr/Yb diagrams for the Pampean arc granitoids. Primitive mantle (PM) values after McDonough and Sun (1995). Black arrows indicate ideal trajectories caused by fluid- and sediment-dominate processes (Gamble et al., 1997).

quartz diorites, those with a clear I-type signature and lower meta-sedimentary imprint, are moderately variable with ϵNd_i values ranging between -2.4 and +1.8 and Sr/Sr_i of 0.704305—0.70808 for a SiO_2 range of 50.93 to 56.84 wt%. This whole-rock isotopic variability is also registered in the scarce available zircon Hf data (a diorite sample from the Puna; Ortiz et al., 2017) with ϵHf_i values varying between -9.5 and -1.2 (n =4) and one datum of +9.1 (Supplementary Material S4). Although there are very scarce isotopic data, such isotopic variance may indicate different contributions of mantle and crustal sources. Therefore, the isotopic variability found in these rocks could be the consequence of either the interaction of diorite magmas with +1.8 ϵNd_i and crustal materials, or derivation from a heterogeneous source such as the lithospheric mantle (e.g., Chapman et al., 2021) likely metasomatized by

sediments or sediments-derived melts as indicated by the high Cs/Sc and Zr/Yb ratios of the studied rocks (Fig. 12). An alternative to the heterogeneous lithospheric mantle could be melting of subducted mélanges (e.g., Castro et al., 2010; Codillo et al, 2018), where dioritic melts can be produced by complete reaction of the bulk mélanges and the peridotite (Castro, 2013; Castro et al., 2021).

On the other hand, the intermediate to acidic granitoids (>60 wt% SiO₂) of the Pampean arc exhibit overlapping isotopic signatures. The dominant hybrid granodiorites (ϵNd_i : -2.5 to -5.2) are comparable to granitoids from the Sierra Norte-Ambargasta batholith, the least hybridized rocks showing stronger I-type affinity (ϵNd_i : -1.8 to -5.9), as well as to the strongly peraluminous granites of the Saldania Belt with a distinctive S-type signature (ϵNd_i : -3.3 to -5.8). They also show partial

overlapping with the youngest strongly peraluminous anatectic granites of the Sierras de Córdoba (ϵNd_i : -4.8 to -6.5), which are unrelated to the arc magmatism. This emphasizes that the compositional endmembers at the source level had enriched isotopic signatures, one represented by a felsic crust, possibly related to the Puncoviscana basement

or its equivalents (ϵNd_i : -3 to -7.7), and the other by a mafic *meta*-igneous source, with either positive or most likely negative ϵNd_i values and heterogeneous, as previously mentioned (enriched lithospheric mantle?). This is also consistent with the strongly variable ϵHf_i values (from -7.6 to +1.9; supplementary material) recorded by these rocks.

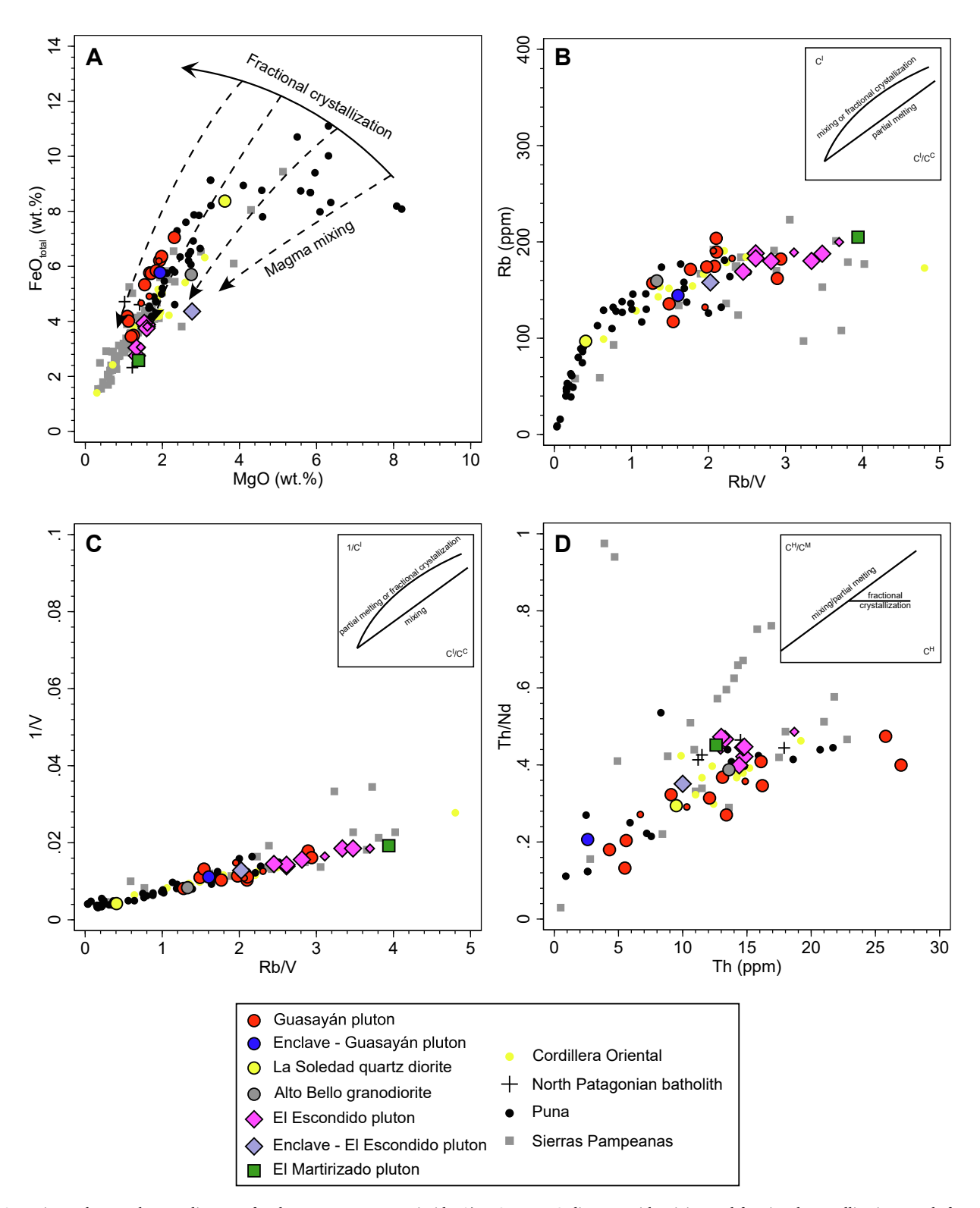


Fig. 13. Major and trace element diagrams for the Pampean arc granitoids. A) FeO vs. MgO diagram with mixing and fractional crystallization trends from Zorpi et al. (1989). B) Rb vs. Rb/V diagram. C) Companion plots of 1/V vs. Rb/V. D) Th/Nd vs. Th diagram. Insets show schematic diagrams of relations between highly and moderately incompatible elements with curves showing melt compositions produced by mixing, fractional crystallization and partial melting processes (Schiano et al., 2010).

9.6. Petrogenetic mechanisms

The hybrid nature of most granitoids of the Pampean arc has been explained by either magma mixing (Suzaño et al., 2015, 2017; Lira et al., 2014; Ortiz et al., 2017; Zandomeni et al., 2021), interaction between juvenile and continental crustal sources (Dahlquist et al., 2016), contamination/assimilation of old continental crust (Iannizzotto et al., 2013; Bellos et al., 2020b, 2024) and partial melting of a heterogeneous lower continental crust (Dahlquist et al., 2016; Bellos et al., 2020b). We use here for the first time, a large compilation of geochemical and isotope data to constrain the main processes that produced the Pampean arc magmatism.

Regarding major element compositions, the roughly linear trends observed in Harker diagrams except for Al_2O_3 and P_2O_5 (Fig. 7) are better explained by magma mixing (e.g., Fourcade and Allegre, 1981; Perugini and Poli, 2012), although crystal fractionation may also generate similar trends as suggested for granitoids from the Sierra Norte Ambargasta batholith (Lira et al., 1997). Furthermore, the positive trend followed by the Pampean granitoids in the FeO vs. MgO diagram (Fig. 13A) argue for mixing processes (Zorpi et al., 1989) as the main magmatic differentiation mechanism. The scatter observed in some diagrams might be caused by heterogeneities at the source level as highlighted by the high compositional variability shown by the least evolved rocks (see for instance the high variation of MgO, FeO, CaO and TiO₂ for very similar SiO₂ contents; Fig. 7) or by chaotic mixing processes resulting in diffusive fractionation (Perugini et al., 2006; Perugini and Poli, 2012).

The roughly negative correlation between ϵNd_i and SiO_2 observed in Fig. 14A, cannot be explained by simple fractional crystallization, instead it rather points to magma mixing or assimilation of crustal material. The observed scatter might also reflect heterogeneities at the source level. Controversially, in the Sr/Sr_i vs. SiO_2 diagram the data depict a roughly subhorizontal trend (Fig. 14B) that would be more coherent with fractional crystallization, and suggests a decouple behaviour of Sr and Sr also show the lowest Sr/Sr_i , that is, a higher

mantle affinity (Fig. 14B), which would also agree with magma mixing or crustal contamination.

Hybridization or magma mixing is also suggested by the major elements relations shown in Fig. 11, in which the Pampean arc granitoids follow very similar trends to those modeled by Patiño Douce (1999) for hybridization between basic tholeiitic magmas and metapelites at low pressure conditions (\leq 5 kbar). These reaction curves illustrate the compositional changes resulting from the interaction of basaltic magmas with crustal melts, where the pressure and relative contributions of crustal components play a key role in the final melt compositions. The curves highlight the addition of basaltic components and the removal of refractory solids, reflecting complex crust-mantle interactions.

The relations of highly incompatible elements with moderately incompatible and compatible elements can be used to track partial melting, fractional crystallization and mixing as differentiation mechanisms (Schiano et al., 2010). Trace element compositions of the Pampean arc granitoids are also consistent with magma mixing as the main differentiation process for these granitoids, as indicated by their hyperbolic trend in Fig. 13B and the linear trend in Fig. 13C, although fractional crystallization may also have played a role (Fig. 13D).

In this work, we have performed simple isotopic mass balance calculations to evaluate the origin of the Pampean arc granitoids from magma mixing processes. For that, we have used two different diorites from the Puna as the most primitive end-members and an average of the younger strongly peraluminous anatectic granites of the Sierras the Córdoba as the felsic crustal end-member, since these latter are the product of the partial melting of the Puncoviscana Series (Rapela et al., 2002). According to this, isotopic compositions of the granitoids from the Guasayán complex could have been generated from the mixing of the dioritic end-member with variable proportions of the felsic crustal component, with this latter mainly varying between ca. 50 and 65 % for the La Soledad quartz diorite and almost 100 % for one sample of the Guasayán pluton (Fig. 14C). Similar conclusions can be achieved for the rest of the Pampean arc granitoids with 25 - 40 % of crustal component for the most primitive rocks and about 90 % for those with a stronger crustal affinity (Fig. 14C).

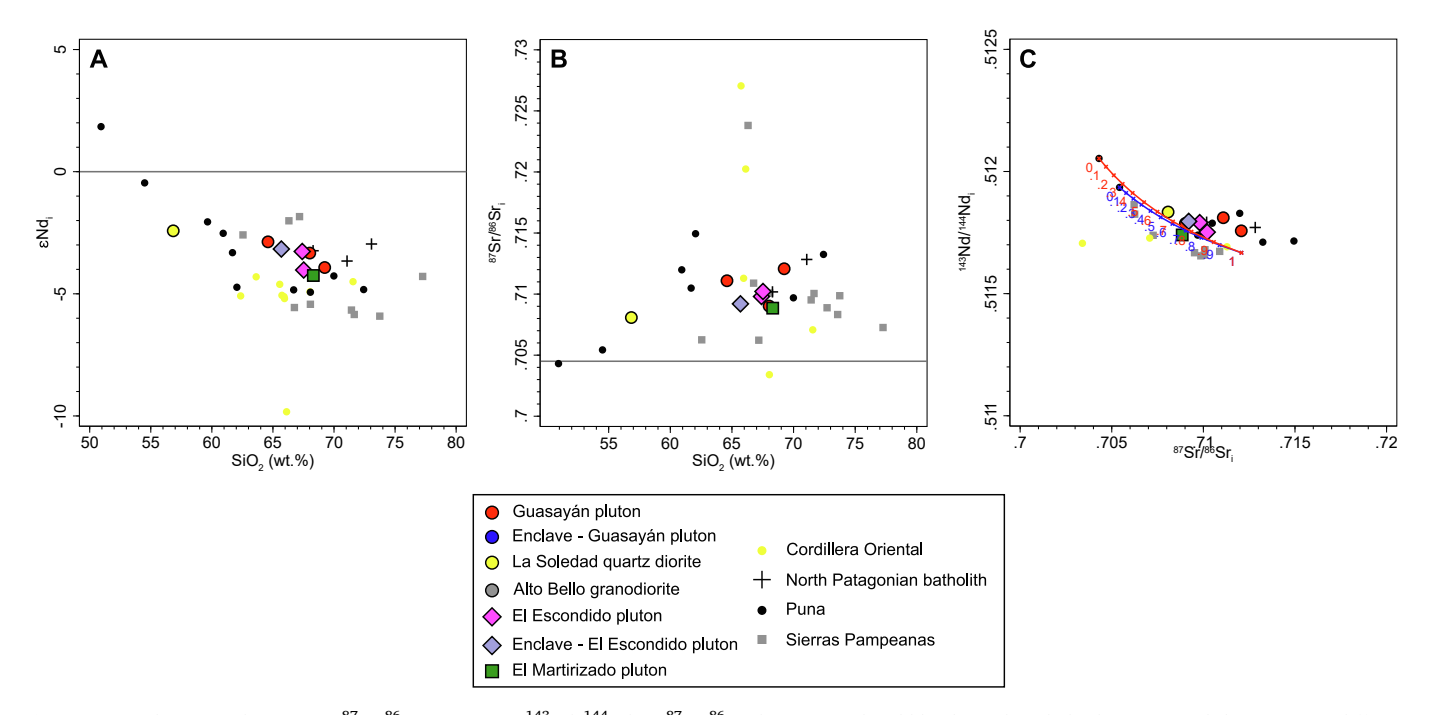


Fig. 14. A) ε Nd_i vs SiO₂ diagram. B) 87 Sr/ 86 Sr_i vs SiO₂. C) 143 Nd/ 144 Nd_i vs 87 Sr/ 86 Sr_i diagram. Red and blue lines show hybridization trends between two different diorites from the Puna (Ortiz et al., 2017) and an average composition of strongly peraluminous anatectic granites from the Sierras de Córdoba (Rapela et al., 2002). Numbers indicate proportions of the felsic component in the mixing model. (For interpretation of the references to colour in this figure legend, the reader is referred to the web version of this article.)

In addition, other processes such as fractional crystallization, peritectic entrainment, crystal accumulation and host-rock assimilation may have played a role at local scale in the different igneous bodies, which could explain some specific trends and the scatter observed in some of the plots. For instance, granitoids from the Guasayán complex show higher TiO₂ and FeO contents for the same SiO₂ content that most of the other Pampean arc granitoids. This may be inherited from the mafic source, since the La Soledad quartz diorite shows the highest TiO₂ contents, but also it could have been generated by preferential entrainment of peritectic ilmenite as suggested by the good correlations between maficity (Fe + Mg) and Ti and V (see Supplementary Material S7) (Clemens and Stevens, 2012; Farina et al., 2012). Nonetheless, the entrainment of peritectic ilmenite may be discarded because good correlations between Ti, V and maficity are also shown by the rest of the Pampean arc granitoids (Supplementary Material S7). Therefore, entrainment of peritectic minerals cannot be responsible for the Fe and Ti enrichment of the Guasayán granitoids but may have been one of the processes that accompanied magma mixing in the diversification of the Pampean arc granitoids.

Assimilation of the country rock may also be responsible for the observed chemical and isotopic variability (Bellos et al., 2020b, 2024). However, partially molten or migmatitic xenoliths, indicative of assimilation processes, have only been described in Cambrian granitoids from Tafi del Valle (Bellos et al., 2020b). Furthermore, genetic relations or interaction between the migmatitic country rocks and the Cambrian granitoids from Tafi del Valle and the Sierra Norte Ambargasta batholith have not been reported either. The apparent absence of clear subhorizontal trends crosscutting the chemical boundaries in the MALI diagram (Fig. 6D) also argue against the assimilation as the main differentiation mechanism (e.g., Frost and Frost, 2008; Moreno et al., 2017). Therefore, it seems that assimilation was a process working at local scale (Suzaño et al., 2017), whereas magma mixing worked likely at the entire arc scale, as suggested by the geochemical and isotopic features of the I-S transitional Pampean granitoids, as well as their mineralogy and widespread textural evidence, such as rapakivi and antirapakivi textures, plagioclase zoning, ocelli and the widespread mafic microgranular enclaves (e.g., Lira and Poklepovic, 2014; Ortiz et al., 2017; Zandomeni et al., 2021).

Therefore, the new data reported here together with the compiled published data point to hybridization or magma mixing (between a heterogeneous dioritic end-member and a peraluminous granitic end-member) as the main mechanism involved in the genesis of the Pampean arc granitoids as previously suggested by other authors (e.g., Lira et al., 2014; Suzaño et al., 2015; Ortiz et al., 2017; Zandomeni et al., 2021), which could operate at the whole arc scale accompanied by other processes with varying degree of significance at the level of the different igneous bodies or complexes.

In a context of arc initiation or subduction initiation, the production of S-type and I-S-type granites or bimodal magmatism can dominate the early stages of arc magmatism due to the fertility of sediments accumulated in a former passive margin (e.g., Ducea et al., 2015b; Clemens and Kisters, 2021). We emphasize here that the zircon age pattern of the strongly peraluminous Alto Bello granodiorite, along with the inheritance detected in most of the hybrid granitoids and the similarities in whole-rock Sr and Nd isotope compositions (Fig. 9), highlights the significance of the Puncoviscana Series both at the source level and as the basement into which these granitoids intruded. Furthermore, subduction erosion could have been a key mechanism for introducing sediments from the forearc (Puncoviscana Series) into the mantle wedge and/or the base of the upper plate (Stern, 2011, 2020; Ducea et al., 2015b), making them available at the source level. In this scenario, the formation of I-type metaluminous diorite magmas could result from the partial melting of the mafic lower crust, the metasomatized subcontinental lithospheric mantle, or diapiric mélanges, whereas the S-type granite magmas formed through the partial melting of the Puncoviscana metasedimentary Series. Finally, we propose here a model for the

Pampean arc, similar to those proposed by Dahlquist et al. (2024) and Santos da Cruz et al. (2024), in which variable degrees of interaction between these contrasting magmas in a long-lasting magmatic system (as revealed by zircon antecrysts of ca. 545 Ma) gave rise to the dominant I-S-type hybrid granitoids. Later, the magmas generated in the Pampean arc would emplace at shallow structural levels under P-T conditions of < 750 °C and < 3 kbar (Lira et al., 2014; Suzaño et al., 2017; Zandomeni et al., 2021).

9.7. The geodynamic scenario of the Pampean orogeny

The Pampean arc domain crops out in the Sierra Norte de Córdoba, Sierra de Guasayán, Puna, Cordillera Oriental and the North Patagonian batholith. This domain underwent low-grade metamorphism and hosts the Cordilleran-type magmatic arc dealt with here. This domain consists mainly of the Ediacaran to early Cambrian Puncoviscana Series that was laid down on a probably extended continental margin (Weinberg et al., 2018) that evolved into active in the early Cambrian. If the Pampean orogeny truly resulted from the collision between the latter margin, that we have inferred was the southern Kalahari margin from detrital zircon evidence (Rapela et al., 2007) and a western continental mass rifted out from Laurentia that we called MARA (Casquet et al., 2012), subduction had to be eastward. This interpretation is strengthened by the fact that in the Sierras de Córdoba domain of the Pampean orogen the Gondwanan sourced Puncoviscana Series is imbricated with the Difunta Correa Sedimentary Sequence, a platform sedimentary succession of Laurentian provenance and of Ediacaran to early Cambrian age (Ramacciotti et al., 2015; Murra et al., 2016; Rapela et al., 2016).

Evidence of right lateral shear during the emplacement of the Pampean Cordilleran magmatic arc suggests that magmatism took place under transpressional conditions inasmuch as magmatism also was coeval with development of upright to west verging folds and dextral shear zones in the Puncoviscana Formation prior to collision (von Gosen and Prozzi, 2010; Iannizzotto et al., 2013). Therefore, the tectonic regime at the time of arc magmatism was one of oblique suduction with strain partitioned in the upper slab, i.e., the Kalahari margin (Fig. 15). Magmatism initiated at ca. 545 Ma (cryptic stage indicated by the age of zircon antecrysts) and continued down to a flare-up of magmatism at 530–535 Ma (Casquet et al., 2018).

According to this model the crust at the time of magmatism consisted of the probably hyper-extended continental crust of the Kalahari craton of Grenvillian age (the Natal-Namaqua belt) and an overlaying clastic wedge, i.e., the Puncoviscana Series (and its equivalent Malmesbury Formation of the Saldania belt; Casquet et al., 2018) (Fig. 15).

In terms of tectonic domains, the Pampean magmatic arc formed on the eastern part of the Puncoviscana clastic wedge, i.e., closer to the continental margin, and came to an end when collision with the MARA block took place (ca. 530 Ma) (Fig. 15). Collision involved the imbrication of the distal part of the Puncoviscana clastic wedge with the platform deposits of eastern MARA, i.e., the Difunta Correa /Ancaján sedimentary succession, which resulted in the formation of a collisional belt in the forearc (as in Fig. 6 of Zhou, 2020). An intervening suture is recognised in the northern Sierra de Córdoba consisting of a dismembered complex of metaperidotite, metapyroxenite, metagabbro, massive chromitite and minor leucogranites that were collectively interpreted as an ophiolite complex (upper mantle and oceanic crust) and hence a relict suture (Ramos et al., 2000; Escayola et al., 2007; Proenza et al., 2008; Martino et al., 2010).

The location of this collisional belt in the forearc is inferred by two facts: 1) The Ancaján / Difunta Correa sedimentary succession dominates westward and is almost absent in the magmatic arc domain; 2) No arc-type magmatism has been recognised in the collisional wedge. The latter was the site of *syn*-tectonic intermediate P/T metamorphism that reached high-grade conditions (750–850 °C) and pressures of 7–8 kbar. Migmatites are widespread in this complex, well recognised in the Sierras de Córdoba (Baldo et al., 1996; Rapela et al., 1998; Otamendi et al.,

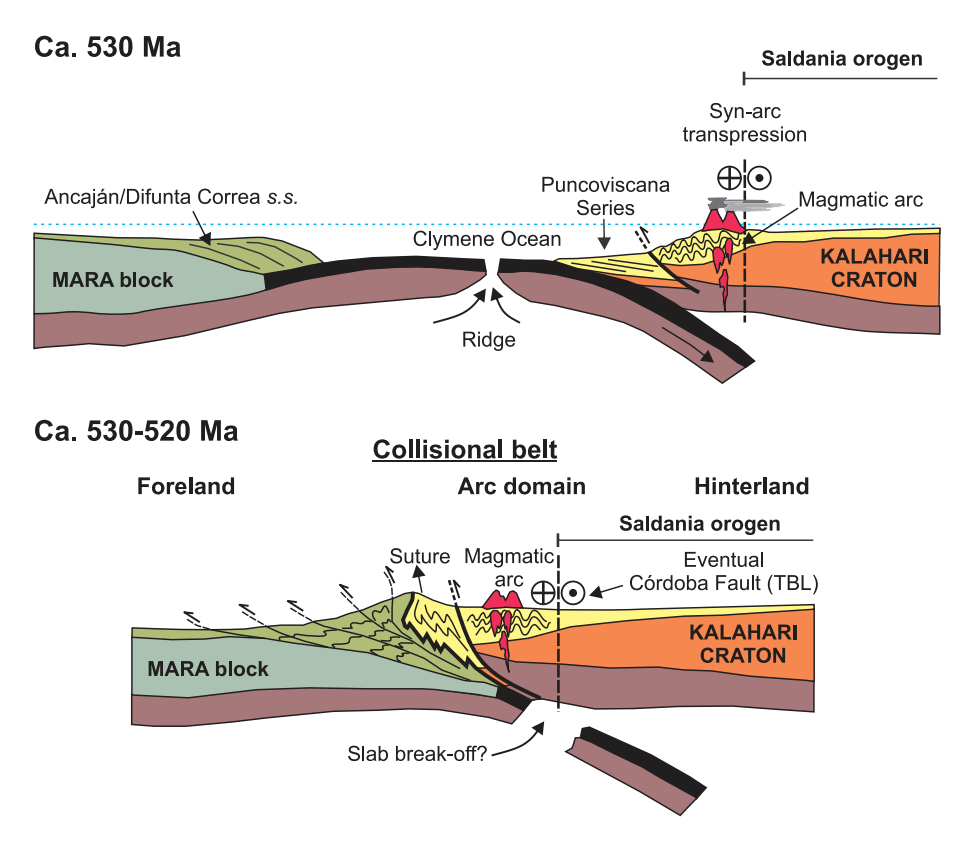


Fig. 15. Sketch of the geodynamic scenario of the Pampean magmatic arc at ca. 530 Ma and its position after collision (ca. 530-520 Ma).

1999). Metamorphism took place between ca. 530 and 520 Ma, i.e., after the main arc magmatic stage. Peak conditions were followed by uplift and intrusion of S-type anatectic granitoids (ca. 550 °C; ca. 3.3 kbar; e. g., Rapela et al., 2002). The collisional belt is separated by a fault zone (the Carapé Fault) from the low-grade metamorphic domain that hosts the Pampean magmatic arc. Therefore, both domains where apart from each other before ca. 520 Ma and juxtaposed later. Remarkably, the low-grade domain did not undergo significant tectonothermal effects after the magmatic arc activity ceased, suggesting that it was not involved to an extent in the collisional wedge. The Pampean inlier preserved well inside the Famatinian belt underwent metamorphism (migmatization) and S-type granitic magmatism between ca. 530 and 520 Ma (Ramacciotti et al., 2024). Therefore, it compares well with the Sierra de Córdoba collisional wedge but was probably in a more distal (westward) location.

The source of heat for metamorphism in the accretionary collision belt remains a matter of debate. One interpretation has invoked ridgesubduction (Simpson et al., 2003; Gromet et al., 2005; Guereschi and Martino, 2014). This hypothesis is appealing but if true, heating should be older than tectonic imbrication because subduction went on after ridge subduction until complete consumption of the Clymene Ocean. However, regional metamorphism was coeval with the development of the main foliation when the metasedimentary succession was inhumated down to ca. 8 kbar, i.e., ca. 30 km depth (Baldo et al., 1996; Casquet et al., 2018). In this regard, some tiny evidence exists of ages between ca. 550 and 540 Ma in zircon overgrowths that could attest to an earlier metamorphism overprinted by the main one (Siegesmund et al., 2010). This cryptic metamorphism could correspond to the early (phase I) Stype granitic magmatism recorded in the Saldania belt (South Africa). We recall here that in our extended model the Saldania belt was formerly juxtaposed to the Pampean belt and that was right laterally displaced along the Transbrasiliano lineament (TBL) (see above) along with the Kalahari craton.

10. Conclusions

The main conclusions of this work can be summarized as follows:

- The Pampean magmatic arc granitoids exhibit a wide compositional range, from metaluminous I-type diorites to strongly peraluminous S-type granites, with the majority showing I-S-type hybrid characteristics.
- 2. Zircon U-Pb geochronology of granitoids from the Sierra de Guasayán indicate crystallization during the main magmatic arc flare-up at ca. 530 Ma. Zircon antecrysts with ages around ~545 Ma, indicate long-lived magmatic systems where early crystallized zircons were recycled into younger magmatic pulses. This may also be extended to the rest of the Pampean magmatic arc.
- 3. Geochemical and isotopic data (Sr-Nd-Hf) highlight the interaction between mafic magmas and felsic magmas, with magma mixing identified as the main process in the generation of the hybrid granitoids, although local-scale processes such as crustal assimilation, fractional crystallization, and peritectic entrainment could also contribute to the geochemical and isotopic diversity observed in the Pampean arc granitoids.
- 4. The Puncoviscana Series played a significant role as a crustal source, evidenced by zircon inheritance patterns and isotopic signatures, and was likely incorporated into the magmatic system through subduction erosion.
- 5. This study highlights the importance of magma mixing in the evolution of subduction-related magmatic arcs and provides a framework for understanding the processes driving continental crust formation in convergent margins.

CRediT authorship contribution statement

Priscila S. Zandomeni: Writing – review & editing, Writing – original draft, Visualization, Investigation, Data curation. **Juan A.**

Moreno: Writing – review & editing, Writing – original draft, Visualization, Supervision, Methodology, Investigation, Data curation, Conceptualization. Matías M. Morales Cámera: Writing – review & editing, Visualization, Investigation. Sebastián O. Verdechia: Writing – review & editing, Visualization, Investigation. Edgardo G. Baldo: Writing – review & editing, Funding acquisition. Juan.A. Dahlquist: Writing – review & editing, Methodology, Investigation, Funding acquisition, Data curation. César Casquet: Writing – review & editing, Visualization, Investigation. Miguel A.S. Basei: Visualization, Methodology. Gilmara Santos da Cruz: Writing – review & editing, Investigation. Carlos W. Rapela: Writing – review & editing, Funding acquisition.

Declaration of competing interest

The authors declare that they have no known competing financial interests or personal relationships that could have appeared to influence the work reported in this paper.

Acknowledgments

Funding was provided by Argentine public grants FONCyT PICT 2020-2891 and SECyT 2023 (33620230100131CB; Universidad Nacional de Córdoba). Funding for open access charge: Universidad de Huelva / CBUA. We sincerely thank two anonymous reviewers for their thorough and constructive feedback, which has significantly improved the quality of our work. We are also grateful to the editor Jan Marten Huizenga for his efficient editorial handling and valuable comments on the final versions of the manuscript. This is the IBERSIMS publication n° 124.

Appendix A. Supplementary data

Supplementary data to this article can be found online at $\frac{\text{https:}}{\text{doi.}}$ org/10.1016/j.gr.2025.09.012.

References

- Aceñolaza, G., Aceñolaza, F., 2007. Insights in the Neoproterozoic–Early Cambrian transition of NW Argentina: facies, environments and fossils in the proto-margin of western Gondwana. Geol. Soc. Lond. Spec. Publ. 286, 1–13. https://doi.org/ 10.1144/SP286.1.
- Aceñaloza, F.G., Toselli, A., 1976. Consideraciones estratigráficas y tectónicas sobre el Paleozoico inferior del Noroeste argentino. In: 2nd Latinoamerican Geologic Congress 2, 755–763 (in Spanish).
- Adams, C.J., Miller, H., Aceñolaza, F.G., Toselli, A.J., Griffin, W.L., 2010. The Pacific Gondwana margin in the late Neoproterozoic-early Paleozoic: Detrital zircon U-Pb ages from metasediments in northwest Argentina reveal their maximum age, provenance and tectonic setting. Gondwana Res. 19, 71–83. https://doi.org/ 10.1016/j.gr.2010.05.002.
- Adams, C.J., Miller, H., Toselli, A.J., Griffin, W.L., 2008. The Puncoviscana Formation of northwest Argentina: U-Pb geochronology of detrital zircons and Rd-Sr metamorphic ages and their bearing on its stratigraphic age, sediment provenance and tectonic setting. Neues Jahrbuch Fur Geologie Und Pälaontologie, Abhandlungen 247, 341–352. https://doi.org/10.1127/0077-7749/2008/0247-0341.
- Annen, C., Blundy, J.D., Sparks, R.S.J., 2006. The genesis of intermediate and silicic magmas in deep crustal hot zones. J. Petrol. 47 (3), 505–539. https://doi.org/ 10.1093/petrology/egi084.
- Anzil, P.A., Martino, R.D., 2009. The megascopic and mesoscopic structure of La Cocha ultramafic body, Sierra Chica of Córdoba, Argentina. J. South American Earth Sci. 28, 398–406. https://doi.org/10.1016/j.jsames.2009.04.012.
- Aparicio González, P.A., Pimentel, M.M., Hauser, N., 2011. Datación U-Pb por LA-ICP-MS de diques graníticos del ciclo pampeano, sierra de Mojotoro, Cordillera oriental. Revista De La Asociación Geológica Argentina 68, 33–38 (in Spanish).
- Aparicio González, P.A., Pimentel, M.M., Hauser, N., Moya, M.C., 2014. U–Pb LA-ICP-MS geochronology of detrital zircon grains from low-grade metasedimentary rocks (Neoproterozoic–Cambrian) of the Mojotoro Range, northwest Argentina. J. S. Am. Earth Sci. 49, 39–50. https://doi.org/10.1016/j.jsames.2013.10.002.Baldo, E.G., Demange, M., Martino, R.D., 1996. Evolution of the Sierras de Córdoba.
- Baldo, E.G., Demange, M., Martino, R.D., 1996. Evolution of the Sierras de Córdoba. Argentina. Tectonophysics 267 (1–4), 121–142. https://doi.org/10.1016/S0040-1951(96)00092-3.
- Baldo, E.G., Rapela, C.W., Pankhurst, R.J., Galindo, C., Casquet, C., Verdecchia, SO., Murra, J.A., 2014. Geocronología de las Sierras de Córdoba: revisión y comentarios. In Geología y Recursos Naturales de la Provincia de Córdoba: Martino, R., Guereschi,

A., Eds. Asociación Geológica Argentina: Córdoba, Argentina, pp. 845–870 (in

- Barbarin, B., 2005. Mafic magmatic enclaves and mafic rocks associated with some granitoids of the central Sierra Nevada batholith, California: nature, origin, and relations with the hosts. Lithos 80 (1–4), 155–177. https://doi.org/10.1016/j. lithos.2004.05.010.
- Beard, J.S., Ragland, P.C., Crawford, M.L., 2005. Reactive bulk assimilation: a model for crust-mantle mixing in silicic magmas. Gondwana Res.. 8, 29–45. https://doi.org/ 10.1016/S1342-937X(05)70283-2.
- Beder, R., 1928. La Sierra de Guasayán y sus Alrededores. Una Contribución a la Geología e Hidrología de la Provincia de Santiago del Estero. Technical Report, Buenos Aires, Ministerio De Agricultura. Dirección General De Minas, Geología e Hidrología. 39, 173 (in Spanish).
- Belcher, R.W., 2003. Tectonostratigraphic evolution of the Swartland region and aspects of orogenic lode-gold mineralization in the Pan-African Saldania Belt, Western Cape, South Africa (Doctoral dissertation, Stellenbosch: Stellenbosch University). http://h dl.handle.net/10019.1/49789.
- Bellos, L.I., Aceñolaza, G.F., Nagle, A.E.A., Díaz-Alvarado, J., Castro, A., Nieva, S.M., López, J.P., Toselli, A.J., 2020a. Petrología, geoquímica y vinculación regional de las unidades neoproterozoicas-cámbricas de la Sierra de Guasayán, Sierras Pampeanas Orientales, Noroeste De Argentina. Acta Geológica Lilloana. 32, 1–26 (in Spanish).
- Bellos, L.I., Boffadossi, M.A., Demartis, M., Nagle, A.E.A., D'Eramo, F., Pinotti, L.P., López, J.P., Muratori, M.E., Coniglio, J.E., Díaz-Alvarado, J., 2024. The Cambrian (Pampean) and early Ordovician (Famatinian) magmatic/migmatitic belt in the Eastern Sierras Pampeanas. Argentina. J. S. Am. Earth Sci. 144, 105032. https://doi. org/10.1016/j.jsames.2024.105032.
- Bellos, L.I., Díaz-Álvarado, J., López, J.P., Rodríguez, N., Nagle, A.E.A., Tassinari, C.C., Altenberger, U., Schleicher, A., 2020b. The juxtaposition of Cambrian and early Ordovician magmatism in the Tafí del Valle area. Characteristics and recognition of Pampean and Famatinian magmatic suites in the easternmost Sierras Pampeanas. J. S. Am Earth Sci. 104, 102878. https://doi.org/10.1016/j.jsames.2020.102878.
- Cashman, K.V., Sparks, R.S.J., Blundy, J.D., 2017. Vertically extensive and unstable magmatic systems: a unified view of igneous processes. Science 355, 1280. https://doi.org/10.1126/science.aag3055.
- Casquet, C., Alasino, P., Galindo, C., Pankhurst, R., Dahlquist, J.A., Baldo, E.G., Ramacciotti, C., Verdecchia, S., Larrovere, M., Rapela, C.W., Recio, C., 2021. The Faja Eruptiva of the Eastern Puna and the Sierra de Calalaste, NW Argentina: U–Pb zircon chronology of the early Famatinan orogeny. J. Iber. Geol. 47, 15–37. https:// doi.org/10.1007/s41513-020-00150-z.
- Casquet, C., Dahlquist, J.A., Verdecchia, S.O., Baldo, E.G., Galindo, C., Rapela, C.W., Pankhurst, R.J., Morales, M.M., Murra, J.A., Fanning, C.M., 2018. Review of the Cambrian Pampean orogeny of Argentina, a displaced orogeny formerly attached to the Saldania Belt of South Africa? Earth Sci.Rev. 177, 209–225. https://doi.org/ 10.1016/j.earscirev.2017.11.013.
- Casquet, C., Rapela, C.W., Pankhurst, R.J., Baldo, E.G., Galindo, C., Fanning, C.M., Dahlquist, J.A., Saavedra, J., 2012. A history of Proterozoic terranes in southern South America: from Rodinia to Gondwana. Geosci. Front. 3 (2), 137–145. https://doi.org/10.1016/j.gsf.2011.11.004.
- Castro, A., 2013. Tonalite-granodiorite suites as cotectic systems: a review of experimental studies with applications to granitoid petrogenesis. Earth Sci. Rev. 124, 68–95. https://doi.org/10.1016/j.earscirev.2013.05.006.
- Castro, A., 2014. The off-crust origin of granite batholiths. Geosci. Front. 5, 63–75. https://doi.org/10.1016/j.gsf.2013.06.006.
- Castro, A., Gerya, T., García-Casco, A., Fernández, C., Díaz-Alvarado, J., Moreno-Ventas, I., Löw, I., 2010. Melting relations of MORB-sediment mélanges in underplated mantle wedge plumes; implications for the origin of Cordilleran-type batholiths. J. Petrol. 51 (6), 1267–1295. https://doi.org/10.1093/petrology/egq019.
- Castro, A., Moreno-Ventas, I., de la Rosa, J.D., 1991. H-type (hybrid) granitoids: a proposed revision of the granite-type classification and nomenclature. Earth Sci. Rev. 31, 237–253. https://doi.org/10.1016/0012-8252(91)90020-G.
- Castro, A., Rodriguez, C., Fernández, C., Aragón, E., Pereira, M.F., Molina, J.F., 2021. Secular variations of magma source compositions in the North Patagonian batholith from the Jurassic to Tertiary: was mélange melting involved? Geosphere 17 (3), 766–785. https://doi.org/10.1130/GES02338.1.
- Chapman, J.B., Shields, J.E., Ducea, M.N., Paterson, S.R., Attia, S., Ardill, K.E., 2021. The causes of continental arc flare ups and drivers of episodic magmatic activity in Cordilleran orogenic systems. Lithos 398–399, 106307. https://doi.org/10.1016/j. lithos.2021.106307.
- Chappell, B.W., 1999. Aluminium saturation in I-and S-type granites and the characterization of fractionated haplogranites. Lithos 46 (3), 535–551. https://doi. org/10.1016/S0024-4937(98)00086-3.
- Chappell, B.W., White, A.J., 2001. Two contrasting granite types: 25 years later. Australian J. Earth Sci. 48 (4), 489–499. https://doi.org/10.1046/j.1440-0952.2001.00882.x.
- Chappell, B.W., White, A.J.R., 1974. Two Contrasting Granite Types. Pac. Geol. 8, 173-174
- Chemale, F., Scheepers, R., Gresse, P.G., Van Schmus, W.R., 2011. Geochronology and sources of late Neoproterozoic to Cambrian granites of the Saldania Belt. Int. J. Earth Sci. 100, 431–444. https://doi.org/10.1007/s00531-010-0579-1.
- Chernicoff, C.J., Zappettini, E.O., Santos, J.O., Godeas, M.C., Belousova, E., McNaughton, N.J., 2012. Identification and isotopic studies of early Cambrian magmatism (El Carancho Igneous complex) at the boundary between Pampia terrane and the Río de la Plata craton, La Pampa province. Argentina. Gondwana Res. 21 (2–3), 378–393. https://doi.org/10.1016/j.gr.2011.04.007.

- Clemens, J.D., Kister, A.F.M., 2021. Magmatic indicators of subduction initiation: the bimodal Goas intrusive Suite in the Pan-African Damara Belt in Namibia. Precambrian Res. 362, 106309. https://doi.org/10.1016/j.gr.2022.05.003.
- Clemens, J.D., Stevens, G., 2012. What controls chemical variation in granitic magmas? Lithos 134–135, 317–329. https://doi.org/10.1016/j.lithos.2012.01.001.
- Clift, P., Vannucchi, P., 2004. Controls on tectonic accretion versus erosion in subduction zones: implications for the origin and recycling of the continental crust. Rev. Geophys. 42, RG2001. https://doi.org/10.1029/2003RG000127.
- Codillo, E.A., Le Roux, V., Marschall, H.R., 2018. Arc-like magmas generated by mélange-peridotite interaction in the mantle wedge. Nat. Commun. 9, 2864. https://doi.org/10.1038/s41467-018-05313-2.
- Cordani, U.G., Brito-Neves, B.B., D'Agrella-Filho, M.S., 2003. From Rodinia to Gondwana: a review of the available evidence from South America. Gondwana Res. 6, 275–283. https://doi.org/10.1016/S1342-937X(05)70976-X.
- Curtis, M.L., 2001. Tectonic history of the Ellsworth Mountains, West Antarctica: reconciling a Gondwana enigma. Geol. Soc. Am. Bull. 113, 939–958. https://doi. org/10.1130/0016-7606(2001)113%3C0939:THOTEM%3E2.0.CO;2.
- Da Silva, L.C., Greese, P.G., Scheepers, R., McNaughton, N.J., Hartmann, L.A., Fletcher, I. R., 2000. U–Pb SHRIMP and Sm–Nd age constraints on the timing and sources of the Pan-African Cape Granite Suite, South Africa. J. Afr. Earth Sci. 30, 795–815. http://h dl.handle.net/10019.1/11119.
- Dahlquist, J.A., Morales Cámera, M.M., Alasino, P.H., Tickyj, H., Basei, M.A.S., Galindo, C., Moreno, J.A., Rocher, S., 2022. Geochronology and geochemistry of Devonian magmatism in the Frontal cordillera (Argentina): geodynamic implications for the pre-andean SW Gondwana margin. Int. Geol. Rev. 64 (2), 233–253. https:// doi.org/10.1080/00206814.2020.1845994.
- Dahlquist, J.A., Morales Cámera, M.M., Moreno, J.A., Basei, M.A.S., Santos da Cruz, G., Oliveira, E.P., 2024. A conceptual model for the evolution of a magmatic system based on U-Pb zircon studies on the Devonian granites of Sierra de San Luis, Argentina. Int. Geol. Rev. 66, 1794–1814. https://doi.org/10.1080/
- Dahlquist, J.A., Verdecchia, S.O., Baldo, E.G., Basei, M.A., Alasino, P.H., Urán, G.A., Rapela, C.W., Campos Neto, M.C., Zandomeni, P.S., 2016. Early Cambrian U-Pb zircon age and Hf-isotope data from the Guasayán pluton, Sierras Pampeanas, Argentina: implications for the northwestern boundary of the Pampean arc. Andean Geol. 43, 137–150. https://doi.org/10.5027/andgeoV43n1-a08.
- Dal Molin, C.N., Fernández, D., Escosteguy, L.D., González, O., Martínez, L., 2003. Hoja Geológica 2766-IV, Concepción. Instituto de Geología y Recursos Minerales, Servicio Geológico Minero Argentino 342, 41 pages (in Spanish). http://repositorio.segemar. gob.ar/handle/308849217/109.
- Debon, F., Le Fort, P., 1983. A chemical-mineralogical classification of common plutonic rocks and associations. Earth and Environ. Sci. Trans. Royal Soc. Edinburgh 73 (3), 135–149. https://doi.org/10.1017/S0263593300010117.
- DeCelles, P.G., Ducea, M.N., Kapp, P., Zandt, G., 2009. Cyclicity in Cordilleran orogenic systems. Nat. Geosci. 2 (4), 251–257. https://doi.org/10.1038/ngeo469.
- DePaolo, D.J., 1981. Trace element and isotopic effects of combined wallrock assimilation and fractional crystallization. Earthand Planetary Sci. Lett. 53 (2), 189–202. https://doi.org/10.1016/0012-821X(81)90153-9.
- DePaolo, D.J., Linn, A.M., Schubert, G., 1991. The continental crustal age distribution: Methods of determining mantle separation ages from Sm-Nd isotopic data and application to the southwestern United States. J. Geophys. Res. Solid Earth 96 (B2), 2071–2088. https://doi.org/10.1029/90JB02219.
- Ducea, M.N., Barton, M.D., 2007. Igniting flare-up events in Cordilleran arcs. Geology 35, 1047–1050. https://doi.org/10.1130/G23898A.1.
- Ducea, M.N., Kidder, S., Chelsey, J.T., Saleeby, J.B., 2009. Tectonic underplating of trench sediments beneath magmatic arcs: the central California example. Int. Geol. Rev. 51, 1–26. https://doi.org/10.1080/00206810802602749.
- Rev. 51, 1–26. https://doi.org/10.1080/00206810802602749.
 Ducea, M.N., Paterson, S.R., DeCelles, P.G., 2015a. High-volume magmatic events in subduction systems. Elements 11, 99–104. https://doi.org/10.2113/GSFLEMENTS.11.2.99.
- Ducea, M.N., Saleeby, J.B., Bergantz, G., 2015b. The architecture, chemistry, and evolution of continental magmatic arcs. Annu. Rev. Earth Planet. Sci. 43, 10–11. https://doi.org/10.1146/annurev-earth-060614-105049.
- Ducea, M.N., Seclaman, A.C., Murray, K.E., Jianu, D., Schoenbohm, L.M., 2017. Mantle-drip magmatism beneath the Altiplano-Puna plateau, central Andes. Nat. Geosci. 10 (6), 435–440. https://doi.org/10.1130/G34509.1.
- Escayola, M., Pimentel, M.M., Armstrong, R., 2007. Neoproterozoic back-arc basin: Sensitive high-resolution ion microprobe U-Pb and Sm-Nd isotopic evidence from the Eastern Pampean Ranges, Argentina. Geology 35 (6), 495–498. https://doi.org/10.1130/G23549A.1.
- Escayola, M.P., van Staal, C.R., Davis, W.J., 2011. The age and tectonic setting of the Puncoviscana Formation in northwestern Argentina: an accretionary complex related to Early Cambrian closure of the Puncoviscana Ocean and accretion of the Arequipa-Antofalla block. J. S. Am. Earth Sci. 32 (4), 438–459. https://doi.org/10.1016/j.jsames.2011.04.013.
- Farina, F., Stevens, G., Gerdes, A., Frei, D., 2014. Small-scale Hf isotopic variability in the Peninsula pluton (South Africa): the processes that control inheritance of source ¹⁷⁶Hf/¹⁷⁷Hf diversity in S-type granites. Contr. Mineral. SPetrol. 168, 1–18. https:// doi.org/10.1007/s00410-014-1065-8.
- Farina, F., Stevens, G., Villaros, A., 2012. Multi-batch, incremental assembly of a dynamic magma chamber: the case of the Peninsula pluton granite (Cape Granite Suite, South Africa). Mineral. Petrol. 106, 193. https://doi.org/10.1007/s00710-012.0224.8
- Favetto, A., Rocha, V., Pomposiello, C., García, R., Barcelona, H., 2015. A new limit for the NW Río de la Plata Craton Border at about 24°S (Argentina) detected by Magnetotellurics. Geol. Acta 13, 243–254.

Foden, J., Elburg, M.A., Dougherty-Page, J., Burtt, A., 2006. The timing and duration of the delamerian orogeny: correlation with the ross orogen and implications for gondwana assembly. J. Geology 114, 189–210. https://doi.org/10.1086/499570.

- Fourcade, S., Allegre, C.J., 1981. Trace elements behavior in granite genesis: a case study the calc-alkaline plutonic association from the Querigut complex (Pyrénées, France). Contr. Mineral. Petrol. 76 (2), 177–195. https://doi.org/10.1007/BF00371958.
- Frimmel, H.E., Basei, M.A., Correa, V.X., Mbangula, N., 2013. A new lithostratigraphic subdivision and geodynamic model for the Pan-African western Saldania Belt, South Africa. Precambrian Res. 231, 218–235. https://doi.org/10.1016/j. precamres.2013.03.014.
- Frost, B.R., Barnes, C.G., Collins, W.J., Arculus, R.J., Ellis, D.J., Frost, C.D., 2001.
 A geochemical classification for granitic rocks. J. Petrol. 42, 2033–2048. https://doi.org/10.1093/petrology/42.11.2033.
- Frost, B.R., Frost, C.D., 2008. A geochemical classification for feldspathic igneous rocks. J. Petrol. 49, 1955–1969. https://doi.org/10.1093/petrology/egn054.
- Gamble, J.A., Christie, R.H., Wright, I.C., Wysoczanski, R.J., 1997. Primitive K-rich magmas from Clark Volcano, southern Kermadec Arc: a paradox in the K depth relationship. Can. Mineral. 35, 275–290.
- González, R.R., Toselli, A.J., 1974. Radimetric dating of igneous rocks from Sierras Pampeanas, Argentina. Rev. Bras. Geocienc. 4, 137–141. https://doi.org/10.25249/ 0375-7536 1974137141
- Goodge, J., 1997. Latest Neoproterozoic basin inversion of the Beardmore Group, Central Transantarctic Mountains, Antarctica. Tectonics 16. https://doi.org/10.1029/ 97TC01417.
- Gresse, P.G., Von Veh, M.W., Frimmel, H.E., 2006. Namibian, (Neoproterozoic) to early Cambrian successions. In: Johnson, M.R., Anhaeusser, C.R., Thomas, R.J. (Eds.), 2006. Geological Society of South Africa, Johannesburg, The Geology of South Africa, pp. 395–420.
- Gromet, L.P., Otamendi, J.E., Miró, R.C., Demichelis, A.H., Schwartz, J.J., Tibaldi, A.M., 2005. The Pampean orogeny: ridge subduction or continental collision. Gondwana 12, 185.
- Gromet, L.P., Simpson, C., 2000. Cambrian orogeny in the Sierras Pampeanas, Argentina: ridge subduction or continental collision. Geol. Soc. Am. Abstr. Programs 32.
- Grosse, P., Bellos, L.I., de los Hoyos, C.R., Larrovere, M.A., Rossi, J.N., Toselli, A.J., 2011.

 Across-arc variation of the Famatinian magmatic arc (NW Argentina) exemplified by I., S-and transitional I/S-type Early Ordovician granitoids of the Sierra de Velasco.

 J. S. Am. Earth Sci. 32, 110–126. https://doi.org/10.1016/j.jsames.2011.03.014.

 Grove, T., Parman, S., Bowring, S., Price, R., Baker, M., 2002. The role of an H2O-rich
- Grove, T., Parman, S., Bowring, S., Price, R., Baker, M., 2002. The role of an H2O-rich fluid component in the generation of primitive basaltic andesites and andesites from the Mt. Shasta Region, N California: Contributions to Mineralogy and Petrology 142, 375–396. https://doi.org/10.1007/s004100100299.
- Guereschi, A.B., Martino, R.D., 2014. Las migmatitas de las Sierras de Córdoba. In: Martino, R.D., Guereschi, A.B. (Eds.), Geología y Recursos Naturales de la Provincia de Córdoba, Relatorio del 19°Congreso Geológico Argentino, Córdoba (in Spanish).
- Hacker, B.R., Kelemen, P.B., Rioux, M., McWilliams, M.O., Gans, P.B., Reiners, P.W., Layer, P.W., Söderlund, U., Vervoort, J.D., 2011. Thermochronology of the Talkeetna intraoceanic arc of Alaska: Ar/Ar, U-Th/He, Sm-Nd and Lu-Hf dating. Tectonics 30, TC1011. https://doi.org/10.1029/2010TC002798.
- Hauser, N., Matteini, M., Omarini, R.H., Pimentel, M.M., 2011. Combined U–Pb and Lu–Hf isotope data on turbidites of the Paleozoic basement of NW Argentina and petrology of associated igneous rocks: Implications for the tectonic evolution of western Gondwana between 560 and 460 Ma. Gondwana Res. 19, 100–127. https:// doi.org/10.1016/j.gr.2010.04.002.
- Hawkesworth, C.J., Gallagher, K., Hergt;, J.M., McDermott, F., 1993. Trace element fractionation processes in the generation of island arc basalts. Philosophical transactions of the Royal Society of London. Series A: Physical and Eng. Sci. 342, 179–191. https://doi.org/10.1098/rsta.1993.0013.
- Hongn, F.D., Tubía, J.M., Aranguren, A., Vegas, N., Mon, R., Dunning, G.R., 2010. Magmatism coeval with lower Paleozoic shelf basins in NW-Argentina (Tastil batholith): constraints on current stratigraphic and tectonic interpretations. J. S. Am. Earth Sci. 29 (2), 289–305. https://doi.org/10.1016/j.jsames.2009.07.008.
- Iannizzotto, N.F., Rapela, C.W., Baldo, E.G., Galindo, C., Fanning, C.M., Pankhurst, R.J., 2013. The Sierra Norte-Ambargasta batholith: late Ediacaran–Early Cambrian magmatism associated with Pampean transpressional tectonics. J. S. Am. Earth Sci. 42, 127–142. https://doi.org/10.1016/j.jsames.2012.07.009.
- Jezek, P., 1990. Análisis sedimentológico de la Formación Puncoviscana entre Tucumán y Salta. El Ciclo Pampeano en el Noroeste Argentino. Serie Correlación Geológica 4, 9–36 (in Spanish).
- Kirsch, M., Paterson, S.R., Wobbe, F., Ardila, A.M.M., Clausen, B.L., Alasino, P.H., 2016. Temporal histories of Cordilleran continental arcs: Testing models for magmatic episodicity. Am. Mineral. 101, 2133–2154. https://doi.org/10.2138/am-2016-5718.
- Kisters, A., Belcher, R., 2018. The Stratigraphy and structure of the western Saldania Belt, South Africa and geodynamic implications. Geology of Southwest Gondwana 387–410. https://doi.org/10.1007/978-3-319-68920-3_14.
- Larrovere, M.A., Casquet, C., Aciar, R.H., Baldo, E.G., Alasino, P.H., Rapela, C.W., 2021.
 Extending the Pampean orogen in western Argentina: New evidence of Cambrian magmatism and metamorphism within the Ordovician Famatinian belt revealed by new SHRIMP U-Pb ages. J. S. Am. Earth Sci. 109, 103222. https://doi.org/10.1016/j.jsames.2021.103222.
- Laurent, O., Martin, H., Moyen, J.F., Doucelance, R., 2014. The diversity and evolution of late-Archean granitoids: evidence for the onset of "modern-style" plate tectonics between 3.0 and 2.5 Ga. Lithos 205, 208–235. https://doi.org/10.1016/j. lithog.2014.06.12.
- Lee, C.T.A., Morton, D.M., Kistler, R.W., Baird, A.K., 2012. Petrology and tectonics of Phanerozoic continent formation: from island arcs to accretion and continental arc

magmatism. Earth Planet. Sci. Lett. 263–264, 370–387. https://doi.org/10.1016/j.

- Lim, H., Nebel, O., Weinberg, R.F., Nebel-Jacobsen, Y., Barrote, V.R., Park, J., Myeong, B., Cawood, P.A., 2023. Lower crustal hot zones as zircon incubators? Inherited zircon antecrysts in diorites from a mafic mush reservoir. In: van Schijndel, V., Cutts, K., Pereira, I., Guitreau, M., Volante, S., Tedeschi, M. (Eds.). Minor Minerals, Major Implications: Using Key Mineral Phases to Unravel the Formation and Evolution of Earth's Crust. Geol. Soc. Lond. Spec. Publ. 537, 411–433. Doi: 10.1144/SP537-2021-195
- Lira, R., Millone, H.A., Kirschbaum, A.M., Moreno, R.S., 1997. Calc-alkaline arc granitoid activity in the Sierra Norte-Ambargasta Ranges, central Argentina. J. S. Am. Earth Sci. 10, 157–178. https://doi.org/10.1016/S0895-9811(97)00013-8.
- Lira, R., Poklepovic, M.F., O'LEary, M.S., 2014. El magmatismo cámbrico en el batolito de Sierra Norte-Ambargasta. In Geología y Recursos Naturales de la Provincia de Córdoba: Martino, R., Guereschi, A., Eds. Asociación Geológica Argentina: Córdoba, Argentina, pp. 183–216 (in Spanish).
- Llambías, E.J., Gregori, D., Basei, M.A., Varela, R., Prozzi, C., 2003. Ignimbritas riolíticas neoproproterozoicas en la Sierra Norte de Córdoba: evidencia de un arco magmático temprano en el ciclo Pampeano? Revista De La Asociación Geológica Argentina 58, 572–582
- Lucassen, F., Becchio, R., Wilke, H.G., Franz, G., Thirlwall, M.F., Viramonte, J., Wemmer, K., 2000. Proterozoic-Paleozoic development of the basement of the Central Andes (18–26°S) a mobile belt of the South American craton. J. S. Am. Earth Sci. 13 (8), 697–715. https://doi.org/10.1016/S0895-9811(00)00057-2.
- Ma, L., Jiang, S.-Y., Hou, M.-L., Dai, B.-Z., 2022. Cretaceous oceanic slab subduction and subsequent flare-up magmatism in the eastern Jiangnan Orogen, South China: evidence from adaktic granites. Gondw. Res. 110, 1–17. https://doi.org/10.1016/j. gr.2022.05.017.
- Martino, R.D., Guereschi, A.B., Anzil, P.A., 2010. Metamorphic and tectonic evolution at 31°36'S across a deep crustal zone from the Sierra Chica of Córdoba, Sierras Pampeanas. Argentina. J. s. Am. Earth Sci. 30, 12–28. https://doi.org/10.1016/j.jsames.2010.07.008.
- McDonough, W.F., Sun, S.S., 1995. The composition of the Earth. Chem. Geol. 120 (3–4), 223–253. https://doi.org/10.1016/0009-2541(94)00140-4.
- Miller, J.S., Matzel, J.E.P., Miller, C.F., Burgess, S.D., Miller, R.B., 2007. Zircon growth and recycling during the assembly of large, composite arc plutons. J. Volcanol. Geotherm. Res. 167, 282–299. https://doi.org/10.1016/j.jvolgeores.2007.04.019.
- Morales Cámera, M.M., Dahlquist, J.A., Basei, M.A., Galindo, C., Neto, M.D.C.C., Facetti, N., 2017. F-rich strongly peraluminous A-type magmatism in the pre-andean foreland Sierras Pampeanas, Argentina: geochemical, geochronological, isotopic constraints and petrogenesis. Lithos 277, 210–227. https://doi.org/10.1016/j. lithos.2016.10.035.
- Moreno, J.A., Baldim, M.R., Semprich, J., Oliveira, E.P., Verma, S.K., Teixeira, W., 2017. Geochronological and geochemical evidences for extension-related Neoarchean granitoids in the southern São Francisco Craton. Brazil. Precambrian Res. 294, 322–343. https://doi.org/10.1016/j.precamres.2017.04.011.
- Murra, J.A., Baldo, E.G., Galindo Francisco, M., Casquet, C., Pankhurst, R.J., Rapela, C. W., Dahlquist, J.A., 2011. Sr, C and O isotope composition of marbles from the Sierra de Ancasti, Eastern Sierras Pampeanas, Argentina: age and constraints for the Neoproterozoic–Lower Paleozoic evolution of the proto-Gondwana margin. Geol. Acta 9, 79–92. https://hdl.handle.net/20.500.14352/42075.
- Murra, J.A., Casquet, C., Locati, F., Galindo, C., Baldo, E.G., Pankhurst, R.J., Rapela, C. W., 2016. Isotope (Sr, C) and U–Pb SHRIMP zircon geochronology of marble-bearing sedimentary series in the Eastern Sierras Pampeanas, Argentina. Constraining the SW Gondwana margin in Ediacaran to early Cambrian times. Precambrian Res. 281, 602–617. https://doi.org/10.1016/j.precamres.2016.06.012.
- Mutti, D.I., 1997. La secuencia ofiolítica basal desmembrada de las sierras de Córdoba. Rev. Asoc. Geol. Argent. 52 (3), 275–285 (in Spanish).
- Omarini, R.H., Sureda, R.J., Götze, H.J., Seilacher, A., Plüger, F., 1999. Puncoviscana folded belt: testimony of late Proterozoic Rodinia fragmentation and the collisional pre-Gondwanic episodes. Int. J. Earth Sci. 88, 76–97. https://doi.org/10.1007/ s005310050247.
- Omil, M., 1992. Geología y geomorfología del basamento de la Sierra de Guasayán, provincia de Santiago del Estero. Doctoral dissertation, Universidad Nacional de Tucumán (in Spanish).
- Ortiz, A., Hauser, N., Becchio, R., Suzaño, N., Nieves, A., Sola, A., Pimentel, M., Reimold, W., 2017. Zircon U-Pb ages and Hf isotopes for the Diablillos intrusive complex, southern Puna, Argentina: crustal evolution of the lower Paleozoic Orogen, southwestern Gondwana margin. J. S. Am. Earth Sci. 80, 316–339. https://doi.org/ 10.1016/j.jsames.2017.09.031.
- Ortiz, A., Suzaño, N., Hauser, N., Becchio, R., Nieves, A., 2019. New hints on the evolution of the Eastern Magmatic Belt, Puna Argentina. SW Gondwana margin: Zircon U-Pb ages and Hf isotopes in the Pachamama Igneous-Metamorphic complex. J. S. Am Earth Sci. 94, 102246. https://doi.org/10.1016/j.jsames.2019.102246.
- Otamendi, J.E., Cristofolini, E.A., Morosini, A., Armas, P., Tibaldi, A.M., Camilletti, G.C., 2020. The geodynamic history of the Famatinian arc, Argentina: a record of exposed geology over the type section (latitudes 27°- 33° south). J. S. Am. Earth Sci. 100, 1–22. https://doi.org/10.1016/j.jsames.2020.102558.
- Otamendi, J.E., Patiño Douce, A.E., Demichelis, A.H., 1999. Amphibolite to granulite transition in aluminous greywackes from the sierra de Comechingones, Córdoba, Argentina. J. Metamorph. Geol. 17, 415–434. https://doi.org/10.1046/j.1525-1314.1999.00208.x.
- Pankhurst, R.J., Rapela, C.W., López de Luchi, M.G., Rapalini, A.E., Fanning, C.M., Galindo, C., 2014. The Gondwana connections of northern Patagonia. J. Geol. Soc. 171 (3), 313–328. https://doi.org/10.1144/jgs2013-081.

Patiño Douce, A.E., 1999. What do experiments tell us about the relative contributions of crust and mantle to the origin of granitic magmas? Geol. Soc. Lond. Spec. Publ. 168 (1), 55–75. https://doi.org/10.1144/GSL.SP.1999.168.01.05.

- Perugini, D., Petrelli, M., Poli, G., 2006. Diffusive fractionation of trace elements by chaotic mixing of magmas. Earth Planet. Sci. Lett. 243 (3–4), 669–680. https://doi. org/10.1016/j.epsl.2006.01.026.
- Perugini, D., Poli, G., 2012. The mixing of magmas in plutonic and volcanic environments: analogies and differences. Lithos 153, 261–277. https://doi.org/ 10.1016/j.lithos.2012.02.002.
- Proenza, J.A., Zaccarini, F., Escayola, M., Cábana, C., Schalamuk, A., Garuti, G., 2008. Composition and textures of chromite and platinum-group minerals in chromitites of the western ophiolitic belt from Pampean Rang es of Córdoba. Argentina. Ore Geology Rev. 33, 32–48. https://doi.org/10.1016/j.oregeorev.2006.05.009.
- Ramacciotti, C.D., Baldo, E.G., Casquet, C., 2015. U–Pb SHRIMP detrital zircon ages from the Neoproterozoic Difunta Correa metasedimentary sequence (Western Sierras Pampeanas, Argentina): provenance and paleogeographic implications. Precambrian Res. 270, 39–49. https://doi.org/10.1016/j.precamres.2015.09.008.
- Ramacciotti, C.D., Casquet, C., Baldo, E., Galindo, C., Pankhurst, R., Verdecchia, S., Rapela, C., Fanning, M., 2018. A Cambrian mixed carbonate-siliciclastic platform in SW Gondwana: evidence from the Western Sierras Pampeanas (Argentina) and implications for the early Paleozoic paleogeography of the proto-Andean margin. International Journal of Earth Sciences 107, 2605–2625. https://doi.org/10.1007/s00531-018-1617-7.
- Ramacciotti, C.D., Casquet, C., Cámera, M.M.M., Murra, J.A., Larrovere, M.A., Dahlquist, J.A., Verdecchia, S.O., Alasino, P.H., Lembo Wuest, C.I., Baldo, E.G., 2024. Cambro-Ordovician stratigraphic record of two distinctive Famatinian belts fringing SW Gondwana: insights from SHRIMP U–Pb zircon ages and geochemistry from the Sierra de Famatina (NW Argentina). Int. J. Earth Sci. (Geol. Rundsch) 113, 1365–1384. https://doi.org/10.1007/s00531-024-02439-1.
- Ramos, V.A., Escayola, M., Leal, P., Pimentel, M.M., Santos, J., 2015. The late stages of the Pampean Orogeny, Córdoba (Argentina): evidence of postcollisional Early Cambrian slab break-off magmatism. J. S. Am. Earth Sci. 64, 351–364. https://doi. org/10.1016/j.jsames.2015.08.002.
- Ramos, V.A., Escayola, M., Mutti, D.I., Vujovich, G.I., 2000. Proterozoic-early Paleozoic ophiolites of the Andean basement of southern South America. Geol. Soc. Am. Spec. 349, 331–350. https://doi.org/10.1130/0-8137-2349-3.331.
- Ramos, V.A., Martino, R.D., Otamendi, J.E., Escayola, M.P., 2014. Evolución geotectónica de las Sierras Pampeanas Orientales. In: Martino, R.D., Guereschi, A.B. (Eds.), Geología y Recursos Naturales de la Provincia de Córdoba. Proceedings of the XIX Congreso Geológico Argentino, Córdoba, Argentina, pp. 965–977 (in Spanish).
- Ramos, V.A., Vujovich, G.I., 1993. The Pampia Craton within Western Gondwanaland. In: Ortega-Gutiérrez, F., Coney, P., Centeno-García, E., Gómez-Caballero, A. (Eds.), Proceedings of The First Circum-Pacific and Circum-Atlantic Terrane Conference. México. 113–116.
- Rapalini, A.E., de Luchi, M.L., Tohver, E., Cawood, P.A., 2013. The South American ancestry of the North Patagonian Massif: geochronological evidence for an autochthonous origin? Terra Nova 25 (4), 337–342. https://doi.org/10.1111/ ter.12043
- Rapela, C.W., Baldo, E.G., Pankhurst, R.J., Saavedra, J., 2002. Cordierite and leucogranite formation during emplacement of highly peraluminous magma: the El Pilón Granite complex (Sierras Pampeanas, Argentina). J. Petrol. 43, 1003–1028. https://doi.org/10.1093/petrology/43.6.1003.
- Rapela, C.W, Pankhurst, R., Casquet, C., Baldo, E., Saavedra, J., Galindo, C. Fanning, C. 1998. The Pampean Orogeny of the southern proto-Andes: Cambrian continental collision in the Sierras de Córdoba. In: Pankhurst, R.J., Rapela, C.W. (eds.), The Proto-Andean margin of Gondwana. Geol. Soc. Lond. Spec. Publ. 142, 181–217. Doi: 10.1144/CSI.SP.1998.142.01.10.
- Rapela, C.W., Pankhurst, R.J., Casquet, C., Dahlquist, J.A., Fanning, C.M., Baldo, E.G., Galindo, C., Alasino, P.H., Ramacciotti, C.D., Verdecchia, S.O., Murra, J.A., Basei, M. A.S., 2018. A review of the Ordovician Famatinian orogeny in southern South America: evidence of lithosphere reworking and continental subduction in the early proto-andean margin of Gondwana. Earth Sci. Rev. 187, 259–285. https://doi.org/10.1016/j.earscirev.2018.10.006.
- Rapela, C.W., Pankhurst, R.J., Casquet, C., Fanning, C.M., Baldo, E.G., González-Casado, J.M., Galindo, C., Dahlquist, J.A., 2007. The Río de la Plata craton and the assembly of SW Gondwana. Earth Sci. Rev. 83 (1–2), 49–82. https://doi.org/10.1016/j.earscirev.2007.03.004.
- Rapela, C.W., Pankhurst, R., 2020. The continental crust of northeastern Patagonia. Ameghiniana 57 (5), 480–498. https://doi.org/10.5710/AMGH.17.01.2020.3270.
- Rapela, C.W., Verdecchia, S.O., Casquet, C., Pankhurst, R.J., Baldo, E.G., Galindo, C., Murra, J.A., Dahlquist, J.A., Fanninge, C.M., 2016. Identifying Laurentian and SW Gondwana sources in the Neoproterozoic to Early Paleozoic metasedimentary rocks of the Sierras Pampeanas: paleogeographic and tectonic implications. Gondwana Res. 32, 193–212. https://doi.org/10.1016/j.gr.2015.02.010.
- Rinehart, L.R., Heckert, A.B., Lucas, S.G., 2022. The utility of probability plotting in palaeobiology. Palaeontology 65, 1–19. https://doi.org/10.1111/pala.12633.
- Rojo-Pérez, E., Linnemann, U., Hofmann, M., Fuenlabrada, J.M., Zieger, J., Fernández-Suárez, J., Andonaegui, P., Sánchez Martínez, S., Díez Fernández, R., Arenas, R., 2022. U-Pb geochronology and isotopic geochemistry of adakites and related magmas in the well-preserved Ediacaran arc section of the SW Iberian Massif: the role of subduction erosion cycles in peri-Gondwanan arcs. Gondwana Res. 109, 89–112. https://doi.org/10.1016/j.gr.2022.04.011.
- Rozendaal, A., Gresse, P.G., Scheepers, R., Le Roux, J.P., 1999. Neoproterozoic to Early Cambrian Crustal Evolution of the Pan-African Saldania Belt, South Africa. Precambrian Res. 97, 303–323. https://doi.org/10.1016/S0301-9268(99)00036-4.

- Santos da Cruz, G., Moreno, J.A., Dahlquist, J.A., Morales Cámera, M.M., Basei, M.A.S., Zandomeni, P.S., 2024. Contributing to understand how Cordilleran batholiths build from detailed geochronology of the Carboniferous Tabaquito batholith, Frontal Cordillera (Argentina). In: Molina, J.F., Cambeses, A., García Casco, A., Montero, P. (Eds.), F. Bea's Work Celebration, Chem. Geol. 662, 122245. Doi: 10.1016/j. chemgeo.2024.122245.
- Scheepers, R., 1995. Geology, geochemistry and petrogenesis of late Precambrian S-, I- and A-type granitoids in the Saldania belt, Western Cape Province. South Africa. J. Afr. Earth Sci. 21, 35–58. https://doi.org/10.1016/0899-5362(95)00087-A.
- Scheepers, R., Schoch, A.E., 2006. The Cape Granite Suite. In: Johnson, M.R., Anhaeusser, C.R., Thomas, R.J. (Eds.), The Geology of South Africa. Geological Society of South Africa/Council for Geoscience, South Africa, pp. 421–432.
- Schiano, P., Monzier, M., Eissen, J.P., Martin, H., Koga, K.T., 2010. Simple mixing as the major control of the evolution of volcanic suites in the Ecuadorian Andes. Contr. Mineral. Petrol. 160, 297–312. https://doi.org/10.1007/s00410-009-0478-2.
- Schoch, A.E., 1975. The Darling granite batholith. Annals University Stellenbosch, Series A.1, Geologie 1, 1–104. http://hdl.handle.net/10019.1/54341.
- Schwartz, J.J., Gromet, L.P., Miró, R., 2008. Timing and duration of the calc-alkaline arc of the Pampean Orogeny: Implication for the Late-Neoproterozoic to Cambrian evolution of Western Gondwana. J. Geol. 116, 39–61. https://doi.org/10.1086/ 524132
- Siégel, C., Bryan, S.E., Allen, C.M., Gust, D.A., 2018. Use and abuse of zircon-based thermometers: a critical review and a recommended approach to identify antecrystic zircons. Earth Sci. Rev. 176, 87–116. https://doi.org/10.1016/j. earscirev.2017.08.011.
- Siegesmund, S., Steenken, A., Martino, R.D., Wemmer, K., López de Luchi, M.G., Frei, R., Presnyakov, S., Guereschi, A., 2010. Time constraints on the tectonic evolution of the Eastern Sierras Pampeanas (Central Argentina). Int. J. Earth Sci. 99, 1199–1226. https://doi.org/10.1007/s00531-009-0471-z.
- Simpson, C., Law, R.D., Gromet, L.P., Miro, R., Northrup, C.J., 2003. Paleozoic deformation in the Sierras de Córdoba and Sierra de las Minas, eastern Sierras Pampeanas. Argentina. J. S. Am. Earth Sci. 15 (7), 749–764. https://doi.org/ 10.1016/S0895-9811(02)00130-X.
- Söllner, F., Höll, R., Miller, H., 1991. U-Pb-Systematik der Zirkone in Meta-Vulkaniten (Porphyroiden) aus der Nördlichen Grauwackenzone und dem Tauernfenster (Ostalpen, österreich). Z. Dtsch. Geol. Ges. 142 (2), 285–299. https://doi.org/ 10.1127/zdgg/142/1991/285.
- Stern, C.R., 2011. Subduction erosion: rates, mechanisms, and its role in arc magmatism and the evolution of the continental crust and mantle. Gondwana Res. 20 (2–3), 284–308. https://doi.org/10.1016/j.gr.2011.03.006.
- Stern, C.R., 2020. The role of subduction erosion in the generation of andean and other convergent plate boundary arc magmas, the continental crust and mantle. Gondwana Res. 88, 220–249. https://doi.org/10.1016/j.gr.2020.08.006.
- Stern, R.J., 2002a. Subduction zones. Rev. Geophys. 40 (4), 1012. https://doi.org/ 10.1029/2001RG000108.
- Stern, R.J., 2002b. Crustal evolution in the East African Orogen: a neodymium isotopic perspective. J. Afr. Earth Sci. 34 (3–4), 109–117. https://doi.org/10.1016/S0899-5362(02)00012-X.
- Stump, E., 1995. The Ross Orogen of the Transantarctic Mountains. Cambridge University Press, Cambridge. 276 pp. Doi: 10.1017/S0954102096230147.
- Suzaño, N., Becchio, R., Nieves, A., Sola, A., Ortiz, A., 2015. Mezcla de magmas en el arco magmático Famatiniano del noroeste de Argentina: ejemplo en el complejo intrusivo Diablillos. Puna Austral. Rev. Mex. Cienc. Geol. 32 (3), 433–454 (in Spanish).
- Suzaño, N., Becchio, R., Sola, A., Ortiz, A., Nieves, A., Quiroga, M., Fuentes, G., 2017. The role of magma mixing in the evolution of the Early Paleozoic calc-alkaline granitoid suites. Eastern magmatic belt, Puna, NW Argentina. J. S. Am. Earth Sci. 76, 25–46. https://doi.org/10.1016/j.jsames.2017.02.008.
- Tatsumi, Y., 2005. The subduction factory: how it operates in the evolving Earth. GSA Today 15 (7), 4–10. https://doi.org/10.1130/1052-5173(2005)015[4:TSFHIO]2.0. CO;2.
- Tibaldi, A.M., Otamendi, J.E., Demichelis, A.H., Barzola, M.G., Barra, F., Rabbia, O.M., Cristofolini, E.A., Benito, M.P., 2021. Early Cambrian multiple-sourced plutonism in the Eastern Sierras Pampeanas, Córdoba, Argentina: Implications for the evolution of the early Paleozoic Gondwana margin. J. S. Am. Earth Sci. 106, 103048. https://doi.org/10.1016/j.jsames.2020.103048.
- Tibaldi, A.M., Otamendi, J.E., Gromet, L.P., Demichelis, A.H., 2008. Suya Taco and Sol de Mayo mafic complexes from eastern Sierras Pampeanas, Argentina: evidence for

- the emplacement of primitive OIB-like magmas into deep crustal levels at a late stage of the Pampean orogeny. J. S. Am. Earth Sci. 26 (2), 172–187. https://doi.org/10.1016/j.isames.2008.03.003.
- Turner, J.C.M., 1960. Estratigrafía de la Sierra de Santa Victoria y Adyacentes (Salta), pp. 1–38
- Verdecchia, S.O., Casquet, C., Baldo, E.G., Pankhurst, R.J., Rapela, C.W., Fanning, C.M., Galindo, C., 2011. Mid- to Late Cambrian docking of the Rio de la Plata craton to southwestern Gondwana: age constraints from U–Pb SHRIMP detrital zircon ages from Sierras de Ambato and Velasco (Sierras Pampeanas, Argentina). J. Geol. Soc. Lond. 168, 1061–1071. https://doi.org/10.1144/0016-76492010-143.
- Villar, L.M., 1975. Las fajas y otras manifestaciones ultrabásicas en la República Argentina y su significado metalogenético. 2nd Cong. Iberoamer. Geol. Eco. 3, 135–156 (in Spanish).
- Villaros, A., Buick, I.S., Stevens, G., 2012. Isotopic variations in S-type granites: an inheritance from a heterogeneous source? Contr. Mineral. Petrol. 163, 243–257. https://doi.org/10.1007/s00410-011-0673-9.
- Villaros, A., Stevens, G., Buick, I.S., 2009. Tracking S-type granite from source to emplacement: clues from garnet in the Cape Granite Suite. Lithos 112, 217–235. https://doi.org/10.1016/j.lithos.2009.02.011.
- Villaseca, C., Barbero, L., Herreros, V., 1998. A re-examination of the typology of peraluminous granite types in intracontinental orogenic belts. Earth Environ. Sci. Trans. R. Soc. Edinb. 89 (2), 113–119. https://doi.org/10.1017/ \$0263593300027045
- Von Gosen, W., McClelland, W.C., Loske, W., Martinez, J.C., Prozzi, C., 2014. Geochronology of igneous rocks in the Sierra Norte de Córdoba (Argentina): implications for the Pampean evolution at the western Gondwana margin. Lithosphere 6 (4), 277–300. https://doi.org/10.1130/L344.1.
- Von Gosen, W., Prozzi, C., 2010. Pampean deformation in the Sierra Norte de Córdoba, Argentina: implications for the collisional history at the western pre-Andean Gondwana margin. Tectonics 29 (2). https://doi.org/10.1029/2009TC002580.
- Watson, E.B., 1996. Dissolution, growth and survival of zircons during crustal fusion: kinetic principles, geological models and implications for isotopic inheritance. Earth Environ. Sci. Trans.R. Soc. Edinb. 87 (1–2), 43–56. https://doi.org/10.1017/ S0263593300006465.
- Watson, E.B., Harrison, T.M., 1983. Zircon saturation revisited: temperature and composition effects in a variety of crustal magma types. Earth Planet. Sci. Lett. 64 (2), 295–304. https://doi.org/10.1016/0012-821X(83)90211-X.
- Weinberg, R.F., Becchio, R., Farias, P., Suzaño, N., Sola, A., 2018. Early Paleozoic accretionary orogenies in NW Argentina: growth of West Gondwana. Earth Sci. Rev. 187, 219–247. https://doi.org/10.1016/j.earscirev.2018.10.001.
- Zandomeni, P.S., Moreno, J.A., Verdecchia, S.O., Baldo, E.G., Dahlquist, J.A., Morales Cámera, M.M., Balbis, C., Benítez, M., Serra-Varela, S., Lembo Wuest, C.I., 2021. Crystallization Conditions and Petrogenetic Characterization of Metaluminous to Peraluminous Calc-Alkaline Orogenic Granitoids from Mineralogical Systematics: The Case of the Cambrian Magmatism from the Sierra de Guasayán (Argentina). Minerals 11, 166. Doi: 10.3390/min11020166.
- Zandomeni, P.S., Verdecchia, S.O., Baldo, E.G., 2017. El metamorfismo de contacto vinculado al magmatismo cámbrico en la Sierra de Guasayán (Santiago del Estero): condiciones P-T y profundidad de emplazamiento. XX Congreso Geológico Argentino. Actas ST5 80–82. San Mieuel de Tucumán (in Soanish.
- Zandomeni, P.S., Verdecchia, S.O., Baldo, E.G., Dahlquist, J.A., Uran, G.M., Alasino, P. H., 2017b. El magmatismo Cámbrico de la Sierra de Guasayán (Provincia de Santiago del Estero) y su Vinculación a la Orogenia Pampeana. XX Congreso Geológico Argentino: Tucumán, Argentina, pp. 308–322 (in Spanish).
- Zhang, J.J., Wang, T., Castro, A., Zhang, L., Shi, X., Tong, Y., Zhang, Z., Guo, L., Yang, Q., Iaccheri, L.M., 2016. Multiple mixing and hybridization from magma source to final emplacement in the Permian Yamatu Pluton, the Northern Alxa Block, China. J. Petrol. 57 (5), 933–980. https://doi.org/10.1093/petrology/egw028.
- Zhou, J.B., 2020. Accretionary complex: Geological records from oceanic subduction to continental deep subduction. Sci. China-Earth Sci. 63 (12), 1868–1883. https://doi. org/10.1007/s11430-019-9652-6.
- Zimmermann, U., 2005. Provenance studies of very low-to low-grade metasedimentary rocks of the Puncoviscana complex, northwest Argentina. Geol. Soc. Lond. Spec. Publ. 246, 381–416. https://doi.org/10.1144/GSL.SP.2005.246.01.16.
- Zorpi, M.J., Coulon, C., Orsini, J.B., Cocirta, C., 1989. Magma mingling, zoning and emplacement in calc-alkaline granitoid plutons. Tectonophysics 157 (4), 315–329. https://doi.org/10.1016/0040-1951(89)90147-9.